Growth–reproduction trade-offs in woody plants are common but changing: a meta-analysis

—

Maciej K. Barczyk*[1], Michał Bogdziewicz[1], Szymon M. Drobniak[2,3], Maria Bogdańska[1], Urszula Eichert[1], Jessie J. Foest[1], Valentin Journé[1,4], Katarzyna Kondrat [1], Jakub Szymkowiak[1,5], Andrew Hacket-Pain[6]

[1] Forest Biology Center, Institute of Environmental Biology, Faculty of Biology, Adam Mickiewicz University, Uniwersytetu Poznańskiego 6, 61-614 Poznań, Poland
[2] Institute of Environmental Sciences, Faculty of Biology, Jagiellonian University, 30-387 Kraków, Poland
[3] School of Biological, Environmental, and Earth Sciences, University of New South Wales, Sydney NSW 2033, Australia
[4] Department of Biology, Faculty of Science, Kyushu University, 819-0395 Fukuoka, Japan
[5] Population Ecology Research Unit, Institute of Environmental Biology, Faculty of Biology, Adam Mickiewicz University, 61-614 Poznań, Poland
[6] Department of Geography and Planning, School of Environmental Sciences, University of Liverpool, Liverpool, L69 7ZX, UK

*Corresponding author: maciejkbarczyk@gmail.com;

Summary

- Growth and reproduction draw on a common resource pool, yet empirical studies of woody plants report widely differing relationships between seed production and growth.
- We synthesized 685 estimates from 78 studies covering 79 woody species, with study locations concentrated at northern temperate latitudes, to test how growth–reproduction correlations vary across time, species, and environments.
- Growth and reproduction measured within the same year were negatively correlated, suggesting an immediate cost of reproduction. Given the limited and uneven taxonomic sampling, phylogenetic patterns in growth–reproduction correlations remain uncertain. The correlations were not systematically related to functional traits or climate. Trade-offs were strongest in species with high interannual variability in seed production and weakened markedly over recent decades in these species.
- Together, these results show that growth–reproduction trade-offs in woody plants are common but not fixed, and that shifts in reproductive variability under environmental change can alter how trees balance growth and reproduction, with consequences for long-term forest functioning.

keywords: growth–reproduction trade-off | cost of reproduction | life-history theory | resource allocation | secondary growth | seed production | tree rings | masting |

Introduction

Individual fitness depends on survival, growth, and reproduction. These functions are constrained by resource-based trade-offs, including the growth–mortality trade-off, the growth–defense trade-off, and the costs of reproduction (Williams, 1966; Obeso, 2002; Dorken *et al.*, 2025; Russo *et al.*, 2020; Cople *et al.*, 2021). In long-lived organisms such as perennial plants, growth-reproduction trade-offs are expected because the allocation of resources is a zero-sum game; reproduction reduces resources available for other functions, such as growth and survival, thereby lowering future fitness returns (Williams, 1966; Dorken *et al.*, 2025). Although the cost of reproduction in plants has been extensively discussed (Dorken *et al.*, 2025; Obeso, 2002; Thomas, 2011), meta-analytic evidence is limited on the extent to which woody plants face a compromise between seed production and somatic growth, and how this varies across species, traits, and habitats (Dorken *et al.*, 2025; Thomas, 2011). Systematic reviews suggest that growth–reproduction trade-offs are widespread (Obeso, 2002; Thomas, 2011), yet case studies report diverse outcomes, including negative (Norton & Kelly, 1988; Woodward *et al.*, 1994; Hadad *et al.*, 2021; Braun *et al.*, 2017), positive (Garcia-Barreda *et al.*, 2021; Alfaro-Sánchez *et al.*, 2015), and absent (Knops *et al.*, 2007; Patterson *et al.*, 2023) correlations between growth and reproduction.

Perennial plants vary widely in their annual allocation to reproduction, offering a test bed for growth–reproduction trade-offs (Norton & Kelly, 1988). Numerous long-lived woody plants show irregular seed production, with years of high, low or absent production, called masting or mast seeding (Bogdziewicz *et al.*, 2024). These among-year shifts in allocation create natural contrasts: years of heavy reproductive investment can be set against lean years to detect growth costs (Norton & Kelly, 1988; Monks *et al.*, 2016). The magnitude of these contrasts varies strongly among species, reflecting differences in interannual variability in reproductive investment, commonly quantified by the coefficient of variation of seed production (CV_p) (Pearse *et al.*, 2020; Journé *et al.*, 2023). Here, we synthesize multi-year measurements of seed production and growth to test how prevalent such trade-offs are across woody plants, and whether their strength depends on phylogeny, functional traits, climate, or temporal change under anthropogenic warming.

Reproductive strategies in plants are shaped by phylogenetic history. Fruit type shows strong conservatism, with phylogeny explaining nearly 80% of the variation between fleshy and dry fruits across 9,370 species from China (Wang *et al.*, 2022). Seed size is similarly associated with evolutionary history, with major divergences in seed mass corresponding to phylogenetic splits across nearly 13,000 species (Moles *et al.*, 2005). Interannual variation in reproduction also carries a phylogenetic signal (Pearse *et al.*, 2020; Qiu *et al.*, 2023; Journé *et al.*, 2023). Together, these findings indicate that reproductive strategies are constrained by ancestry. Consequently, woody plants are expected to be evolutionary constrained in the magnitude of seed production and growth potential, resulting in weaker or stronger allocation trade-offs depending on lineage

(Pearse *et al.*, 2020; Journé *et al.*, 2023; Dorken *et al.*, 2025).

Functional traits capture physiological and morphological strategies that influence growth, survival, and reproduction (Violle *et al.*, 2007; Adier *et al.*, 2014; Díaz *et al.*, 2016). Tree life histories are commonly organized along two major axes: a fast-slow continuum reflecting the growth–survival trade-off and a stature-recruitment axis distinguishing tall, long-lived species with large seeds from shorter-lived species producing numerous small seeds (Rüger *et al.*, 2018; Kambach *et al.*, 2022). Traits associated with acquisitive strategies, including high SLA and low wood density, are also commonly associated with the production of many small seeds, whereas conservative species tend to produce fewer, larger seeds (Bogdziewicz *et al.*, 2023). These relationships produce contrasting expectations for growth-reproduction trade-offs. Dense-wooded species with large seeds may experience greater growth costs because of their reproductive investment (Qiu *et al.*, 2022; Bogdziewicz *et al.*, 2023). Alternatively, under the stature-recruitment axis, tall species with large seeds may incur lower reproductive costs because they invest relatively less in recruitment (Rüger *et al.*, 2018; Kambach *et al.*, 2022).

Spatial variation in temperature and precipitation often mediates reproductive allocation and growth, thereby potentially influencing the apparent strength of trade-offs between them (Hulshof *et al.*, 2012; Shestakova *et al.*, 2021; Hacket-Pain *et al.*, 2018). Across biomes, reproductive allocation tends to increase from cold to warm regions (Journé *et al.*, 2022; Ward *et al.*, 2025). Within species, seed production is also often higher in warmer parts of species' ranges. For example, North American tree fecundity peaks in the warm and moist southeastern United States (Sharma *et al.*, 2022). Parallel patterns emerge for growth. Trees in the tropics grow twice as fast as in temperate and boreal biomes (Locosselli *et al.*, 2020), and within species growth is generally faster at warmer sites (Perret *et al.*, 2024), except where water limitation prevails (Klesse *et al.*, 2024). Similarly, low precipitation and high evaporative demand are associated with stronger negative correlations between growth and reproduction (Hulshof *et al.*, 2012; Hacket-Pain *et al.*, 2017). Together, these findings suggest that accounting for local climate is needed to understand growth–reproduction trade-offs: warm and moist conditions may produce apparent positive associations between growth and reproduction, whereas hot and dry climates are expected to strengthen trade-offs through resource limitation.

Climate change affects resource allocation to reproduction and growth (Etzold *et al.*, 2020; Hacket-Pain & Bogdziewicz, 2021; Clark *et al.*, 2021). Direct effects of warming and moisture limitation often reduce both seed production and growth (Sharma *et al.*, 2022; Klesse *et al.*, 2024; Perret *et al.*, 2024), yet plant responses in many systems appear to maintain reproduction at the expense of growth (Dohrenbusch *et al.*, 2002; Rowland *et al.*, 2018; Bogdziewicz *et al.*, 2020; Szymkowiak *et al.*, 2026). In European beech, warming has shifted reproduction towards more frequent seed crops, depleting stored reserves and causing a ~28% decline in mean radial growth (Hacket-Pain *et al.*, 2025). That change was associated with a weakening of the negative growth–reproduction correlation because, in poor seed years, trees with depleted reserves cannot mount strong growth responses (Hacket-Pain *et al.*, 2025). Experimental evidence supports this

mechanism, for example, *Picea abies* maintained allocation to reproduction at the expense of growth under experimental drought in Germany (Hesse *et al.*, 2021). Alternative mechanisms can also relax trade-offs when resource inputs increase through nitrogen and CO_2 fertilization. Rising atmospheric CO_2 can enhance photosynthetic productivity, resulting in increased wood production and reproductive output (e.g., FACE experiments on oaks) (Norby *et al.*, 2024; Esquivel-Muelbert *et al.*, 2025; Jablonski *et al.*, 2002). Long-term nitrogen addition often increases aboveground wood biomass and seed production (Magill *et al.*, 2004; Bogdziewicz *et al.*, 2017). Anthropogenic change can alter not only the magnitude of demographic rates but also the relationships among them, with particularly strong indirect effects expected in masting species where interactions among resource reserves, growth, and intermittent large seed crops are pronounced (Sala *et al.*, 2012; Han *et al.*, 2017; Hacket-Pain *et al.*, 2017).

Interannual variation in reproductive allocation raises the question of whether growth–reproduction trade-offs operate within years or emerge across years (Knops *et al.*, 2007; Pearse *et al.*, 2016). Resource-budget models of masting predict that reproduction draws on reserves accumulated in previous years, while reserve replenishment after mast events can compete with other carbon sinks such as growth (Isagi *et al.*, 1997; Kabeya *et al.*, 2017, 2021; Kelly *et al.*, 2025). Because reproduction is temporally autocorrelated (Koenig *et al.*, 2003; Foest *et al.*, 2025), high reproductive output in a given year generates a null expectation of reduced reproduction—and thus relatively higher growth—both in the preceding and the following year. Under this expectation, elevated growth in the year preceding and following mast events simply reflects low reproductive investment and associated growth release. Failure to observe elevated growth in the year following mast events represents a deviation from that null expectation and is consistent with delayed costs of reproduction expressed after reproductive investment. Empirical support for such lagged costs is mixed: some studies report reduced subsequent growth or storage following reproduction (Obeso, 2002; Sala *et al.*, 2012), whereas others find that trade-offs are largely confined within the same year (Hadad *et al.*, 2021; Hacket-Pain *et al.*, 2017). Explicitly accounting for null expectations imposed by reproductive autocorrelation is therefore important for correctly interpreting temporal growth–reproduction relationships and for linking allocation dynamics with demographic performance (Hacket-Pain *et al.*, 2018).

To disentangle these mechanisms, we compiled evidence from studies that jointly measured interannual seed production and aboveground, somatic growth across woody plants. We tested five hypotheses related to a broad context of factors that can influence trait trade-offs, including phylogenetic history, functional trait syndromes, spatial variation, and climate-driven effects. (1) Carry-over effects: growth-reproduction trade-offs are strongest within years, but negative effects on growth are expected in the year following high reproductive investment. (2) Phylogeny: trade-off strength is phylogenetically structured, with some lineages showing consistently stronger allocation conflicts. (3) Traits: functional traits mediate allocation patterns; species with conservative syndromes (dense wood, low SLA) exhibit higher reproductive allocation (Qiu *et al.*, 2022; Bogdziewicz *et al.*, 2023), so they should pay larger growth costs reflected in

stronger negative growth–reproduction correlations. Alternatively, tall species with large seeds should display weaker trade-off correlations under the stature–recruitment axis of life history variation (Rüger *et al.*, 2018; Kambach *et al.*, 2022). (4) Climate: the trade-off depends on local climate, weakening under warm–moist conditions that promote resource accumulation and strengthening under hot–dry conditions that increase carbon and water limitation. (5) Reproductive variability and time: growth-reproduction trade-offs are stronger in species with high interannual variability in seed production (high CV_p), reflecting large, episodic reproductive investments that impose greater demands on resources (Norton & Kelly, 1988), but weaken over time under anthropogenic change as more frequent seed years and rising resource inputs (elevated CO_2, nitrogen deposition) decouple annual reproductive effort from short-term growth responses.

Materials and Methods

Meta-analysis To identify relevant studies, we conducted keyword searches in Web of Science and Scopus following the PRISMA guidelines (Preferred Reporting Items for Systematic Reviews and Meta-Analyses); (O'Dea *et al.*, 2021). We evaluated three different combinations of terms related to growth and reproduction (Table S1) inspired by two systematic reviews on the cost of reproduction in plants (Obeso, 2002; Thomas, 2011) and the referenced studies incorporated in our meta-analysis. We applied the final search string on 30 March 2024 including:

> (reproduction OR seed OR seeds OR fruit* OR cone* OR acorn*) AND ("tree growth" OR ring*) AND (tree* OR shrub*)

Given the large number of studies reporting growth (>10,000, Table S1) in non-woody plants, we restricted the search to woody species by using "tree growth" instead of "growth". We also limited the search to trees and shrubs by including these terms directly in the string.

The search yielded 3,449 and 3,111 documents from Web of Science and Scopus, respectively. To streamline the process of literature screening we used Rayyan QCRI (https://rayyan.ai/). After removing duplicates (2,015), we screened abstracts of 4,545 articles, and classified 110 papers for full-text evaluation. That classification was based on a previously constructed decision tree inspired by studies from two systematic reviews (Fig. S1). We also included data from the before-mentioned systematic reviews (Obeso, 2002; Thomas, 2011) and studies cited in recent publications, resulting in a total of 146 publications eligible for data extraction (Fig. S2). Studies on orchard trees and cultivated species were excluded due to the possible bias caused by horticultural selection (Fig. S1).

Out of the 146 articles reporting both annual reproduction and annual growth in woody plants, we positively classified 78 studies based on assessment of the full text. Sixty eight studies that did not contain reliable data on either growth or reproduction, or did not report appropriate statistical tests between them were excluded. In case of studies lacking formal

statistical analyses or raw data suitable for our analysis, we contacted 14 authors asking for the missing data. As five research groups shared their data on six species, we were able to include additional data representing over 60 tree populations. We extracted all lagged effects of reproduction on growth when reported.

We extracted data combining somatic growth and reproduction over multiple years, with a few exceptions for studies based on one year of measurements. Most studies used secondary growth and seed production, but in the final analysis, we also included 13 studies on primary growth and physiological measurements, and 6 studies that measured flower production instead of seed production (Fig. S3). Excluding these studies (based on less frequent categories of growth or reproduction measurement) did not change the qualitative outcome of the analyses despite statistically significant differences in effect sizes among growth measurement methods (Fig. S4, Fig. S5, Table S2,Table S3).

In total, we compiled a dataset of 685 observations (species × population × time-lag effect) from 78 studies containing data on reproduction and growth of trees and other woody plants. We also extracted available effect sizes that were reported in the studies, but were not included in the final analysis, e.g. time lags exceeding one year, correlations based on flower numbers or female individuals only (70 extra effect sizes). Given that seed production in some species (e.g. *Pinus pinea* L. (Garcia-Barreda *et al.*, 2021)) extends over multiple years we classified correlations between time lags in respect to the species' natural history. For example, for *Pinus pinea*, *Pinus palustris* and *Cedrus atlantica* we chose the year of seed filling as the ecologically relevant year to be correlated with growth.

To standardize data for the meta-analysis, we first transformed all reported effect sizes to Pearson's correlation coefficient (r) using test-specific formulas (Table S4). We then converted r to Fisher's Z-scores (Z_r) using

$$Z_r = \frac{1}{2} \ln\left(\frac{1+r}{1-r}\right).$$

The sampling variance of each effect size was calculated as

$$V_{Z_r} = \frac{1}{n-3}.$$

For most observations (97%), the sample size (n) was equivalent to the number of years for which reproduction and growth were correlated. In case of growth-reproduction comparisons that used different statistical tests from correlations, we used the number of years or the number of individuals as the respective sample size. If the sample size was less than four, the observation was excluded from the analysis.

Climate data We extracted mean annual temperature (MAT [°C]), mean annual precipitation (MAP [cm]), minimum temperature of coldest month and maximum temperature of warmest month for each unique study location (Fig. 1A), based on monthly values of temperature and

precipitation (1970 to 2000) from the corresponding 2.5 minute grid cell in the WorldClim2 dataset (Fick & Hijmans, 2017). The extracted values of MAT and MAP were plotted in a Whittaker biome diagram (Fig. 1C) using the *plotbiomes* package (Stefan & Levin, 2025). In addition, we extracted monthly data on vapor pressure deficit (VPD) between 1950 and 2020 for all corresponding locations using *TerraclimateR package v.0.1.0* (Abatzoglou *et al.*, 2018).

Functional traits and masting metrics We compiled functional trait data from publicly available datasets (Kattge *et al.*, 2020; Chave *et al.*, 2009). We filtered the list of species according to the World Checklist of Vascular Plants (WCVP) (Brown *et al.*, 2023). Then we compiled data on species-specific functional traits related to the fast-slow continuum and defined by the global trait analysis (Díaz *et al.*, 2016; Reich, 2014). We selected specific leaf area (SLA), wood density, seed mass, and plant height as potential predictors of the growth-reproduction trade-off. In case of SLA, seed mass and plant height, we were able to obtain the complete data for all 79 species, whereas wood density was available for 61 species. Given the evolutionary conservatism in wood density (Mo *et al.*, 2024), we averaged this trait's values at the genus level for the remaining 18 species. We log-transformed all trait values to approximate a normal distribution, and to facilitate comparisons we scaled and centered these values prior to the analysis.

To obtain the coefficient of variation of seed production (CV_p), we filtered MASTREE+, a global database of annual records of population-level reproductive effort (Hacket-Pain *et al.*, 2022; Foest *et al.*, 2024). We estimated species-level CVp using time series of at least five years from a minimum of five distinct populations per species. Across the 48 species for which we were able to extract the mean CVp, these estimates were based on a mean of 26.8 population-level time series per species (Fig. S6). If information on population-specific seed production variability (CV_p) was reported in the study (11 species), we gave it priority over the value derived from MASTREE+.

Analysis All data analysis was performed in R v. 4.5.1 (R Core Team, 2024). We used the multilevel comparative meta-analysis approach that involves phylogenetic, interspecific, and intraspecific variance partitioning (Pottier *et al.*, 2024). We built our models using the *rma.mv* function in the *metafor* package v.4.8-0 (Viechtbauer, 2010). First, we adapted the time-calibrated phylogeny of plants from Zanne *et al.* (2014) to build our phylogenetic tree. Second, based on our species list, we built a synthetic tree using the Open Tree of Life with the *rotl* package v.3.1.0 (Michonneau *et al.*, 2016) and calculated the distance between branches using Grafen's method. This allowed us to identify synonyms in both phylogenetic trees and bind missing species to the nodes of the closely related species in the time-calibrated phylogenetic tree. Finally, we built the correlation matrix of phylogenetic relatedness under Brownian motion with the *ape* package v.5.8-1 (Paradis & Schliep, 2019) for both phylogenetic trees. We used the phylogenetic correlation matrix derived from the time-calibrated phylogeny of Zanne *et al.*

(2014) in all primary analyses. As a sensitivity analysis, we refitted each model using the Open Tree of Life topology with Grafen-assigned branch lengths. Corresponding model outputs based on both phylogenies are provided in the Supplementary Information (see Fig. S4 and Fig. S5 for the tree comparison). We used *orchaRd* package v.2.0 to plot the results from the *rma* models (Nakagawa *et al.*, 2023).

We fitted phylogenetically informed multilevel random-effects meta-regression models using restricted maximum likelihood. Fisher's Z was used as the response variable, and its sampling variance was supplied to the model for each effect size. The models therefore accounted for sampling uncertainty separately from residual heterogeneity. Non-independence was represented by random effects for phylogenetically structured species identity, study identity, and effect-size identity.

We initially fitted null models with alternative random-effects structures, including study, population, species, effect-size identity, and phylogenetic relatedness. Population identity accounted for effectively no additional variance and was therefore omitted; all subsequent models used the same retained random-effects structure. Fixed effects were interpreted using their estimated coefficients and 95% confidence intervals, with an effect considered statistically supported when its confidence interval did not overlap zero. Total residual heterogeneity was summarized using I^2, and the variance components were used to describe how the estimated heterogeneity was distributed among phylogeny, study, and effect-size identity.

To test whether growth-reproduction trade-offs occur in woody plants worldwide, we fitted a model with time lags included as the model predictors (n = 685). The models tested whether effect sizes (Fisher's Z) differed from zero for correlations measured in year t (a), one-year lags $t-1$ (b), and one-year lags $t+1$ (c) (Fig. 2A). We also quantified the relationship between growth and reproduction correlation within-year with the lagged correlations. To do so, we fitted an *rma* model using the within-year Z-scores as response, and the lagged correlations ($t-1$ and $t+1$) as predictors. This analysis included 172 observations representing 51 species.

In further analyses, we restricted the dataset to within-year correlations (t; a; $n = 308$). We then tested for a phylogenetic signal in the trade-off expression. To this end, we averaged the Z-score at the species level and then calculated Pagel's λ (lambda) and Blombergs' K (Paradis & Schliep, 2019). Because the relatively small and unevenly sampled set of species could influence estimates of phylogenetic signal, we also calculated both metrics for the species-level functional traits included in our analyses: seed mass, wood density (averaged from the genus-level data in 18 species according to the description from the previous paragraph), specific leaf area (SLA), and plant height (Table S5). This allowed us to assess whether phylogenetic structure could be recovered for other traits within the same set of species and using the same phylogeny.

To assess how climate and functional traits modulate growth-reproduction trade-offs, we fitted a multilevel comparative model. Predictors included mean annual temperature (MAT), mean annual precipitation (MAP) and mean vapor pressure deficit (VPD) as key climatic variables, and specific leaf area (SLA), seed mass, plant height, and wood density as relevant functional

traits. We also tested minimum temperature of the coldest month and maximum temperature of the warmest month as alternative measures of temperature extremes. Because both variables were strongly correlated with MAT ($r > 0.78$), they were not included together with MAT in the final model to avoid collinearity among the climatic predictors.

Finally, we fitted a model to test how trade-offs in species characterized by variable CV_p of seed production have changed over recent decades. To do so, we extracted the final year of the study for each observation and fitted a model that included the final year of the study, the average species-specific CV_p of seed production, and their interaction as predictors.

To assess whether the temporal pattern could be driven by changes in the species represented across the study period, we evaluated the sensitivity of the year $\times$ CVp interaction to taxonomic composition by sequentially refitting the model after excluding all (often multiple) observations for each species and each genus represented in the analysis.

We assessed potential publication bias using two methods recommended by Nakagawa *et al.* (2022). Specifically, we plotted a funnel plot with Z-scores and performed multilevel meta-regressions with standard error and sampling variance as fixed predictors of effect size. Visual inspection of the funnel plot suggests that there is no publication bias (Fig. S7). Likewise, the meta-regressions revealed that there is no bias related to studies with small sample sizes as both sampling variance and standard error were non-signifcant predictors of the effect size (Fisher's Z).

Results

Our meta-analysis of 78 studies, 79 species (Fig. 1), and 685 effect sizes across time lags shows that the strength and sign of growth-reproduction correlations depend on their temporal alignment (Fig. 2A,B, Table S6, Table S7). When growth and reproduction were correlated in the same year, the pooled effect size was negative (effect size = −0.231, 95% CI = [−0.362, −0.1], N = 308, see also Fig. 1B), consistent with the within-year trade-offs between growth and reproduction (and across all applied models). Hereafter, we refer to negative growth–reproduction correlations as trade-offs, following their common interpretation as signatures of allocation constraints, while acknowledging that the underlying evidence is correlational (see Discussion).

Growth in year $t-1$ was positively but not significantly associated with reproduction in year t in the primary model using the time-calibrated phylogeny (estimate = 0.108, 95% CI = [−0.026, 0.242], p = 0.11, N = 199; Fig. 2B, Table S6). The corresponding association was positive and statistically significant in the sensitivity model based on the synthetic phylogenetic tree from Open Tree of Life (estimate = 0.143, 95% CI = [0.088, 0.198], $p < 0.0001$; Fig. S8, Table S7). Thus, the direction of the preceding-year association was consistent, although its statistical support depended on the phylogeny used. The expectation that years preceding high reproductive output tend to be characterized by low reproductive investment and, thus, relatively higher growth (Fig. 2B) is further supported by the results from the models testing the lagged and unlagged correlations between effect sizes within observation. This association was strongest in populations with stronger within-year trade-offs (Fig. 2C, Table S8, Table S9), consistent with reproductive autocorrelation generating strong growth contrasts between years of reproductive suppression and preceding low-investment years; particularly in populations with strong growth–reproduction trade-offs. In contrast, reproduction in year t was not associated with growth in year $t+1$ (effect size = 0.007, 95% CI = [−0.128, 0.142], p = 0.92, N = 178; Fig. 2B, Table S6), and regardless of the phylogeny used (Table S7). The absence of a positive association contrasts with the expectation of elevated growth in years adjacent to high reproductive output, indicating an asymmetry around reproductive events, reflected also in within-population correlations (Fig. 2D, Table S8, Table S9). Such a pattern is consistent with delayed costs of reproduction expressed through constrained post-reproductive growth.

Pagel's λ and Blomberg's K gave different numerical results for species-level mean growth-reproduction correlations ($\lambda < 0.001$, p = 1; K = 0.016, p = 0.004; Fig. 3). Because the analysis included only 79 species sampled unevenly across the woody-plant phylogeny, these values cannot reliably assess or bound phylogenetic signal and are reported descriptively. Across the sampled tree, positive and negative effect sizes were interspersed within most major clades and varied markedly within several genera (Fig. 3). Even within genera for which a larger number of species were sampled, such as *Quercus*, *Pinus*, and *Fagus*, the direction and magnitude of effects vary widely among species. Some adjacent taxa differ sharply in effect size, indicating contrasting growth–reproduction correlations despite close evolutionary relatedness. Within

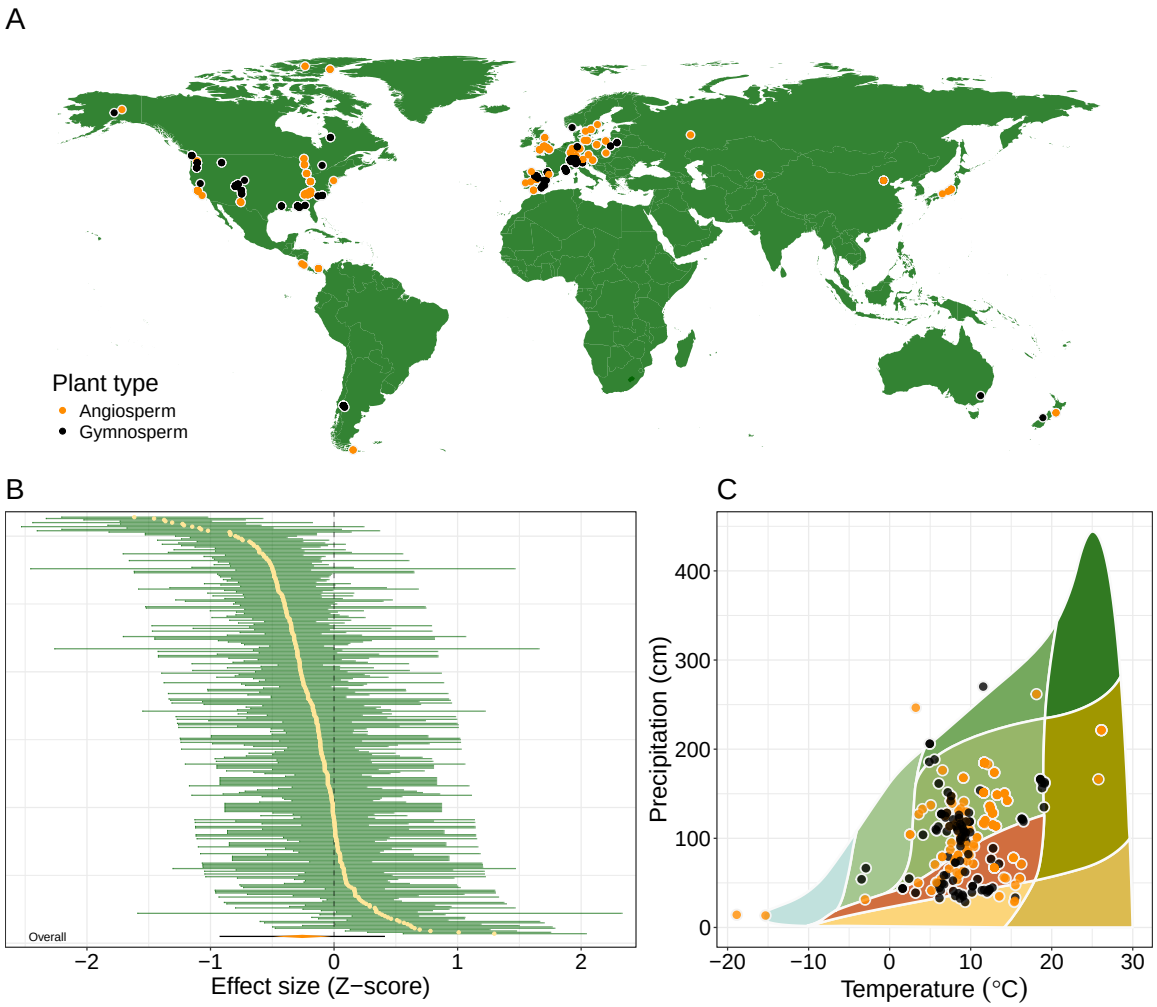


Figure 1: Data distribution and effect size. (A) The location of population-level observations of growth-reproduction correlations. (B) Population-level effect sizes (Z-scores, see Methods) for the relationship between reproduction and growth in the same year (t) with associated 95% confidence intervals (for lagged effects and their framework see Fig. 2A,B). The yellow points indicate the mean of each effect size. The estimated effect size of the null model with the confidence (orange line) and prediction intervals (black line) is shown below (k = 308 observations and $n_{species}$ = 79). (C) Whittaker biome plot with observations distributed along mean annual temperature [°C] and mean annual precipitation [cm]. Orange points indicate species belonging to angiosperms, while black points indicate species belonging to gymnosperms. Background colors refer to the Whittaker Biome classification ranging from tundra (pale blue) through temperate forests in the middle to tropical seasonal and tropical rain forest (olive and dark green).

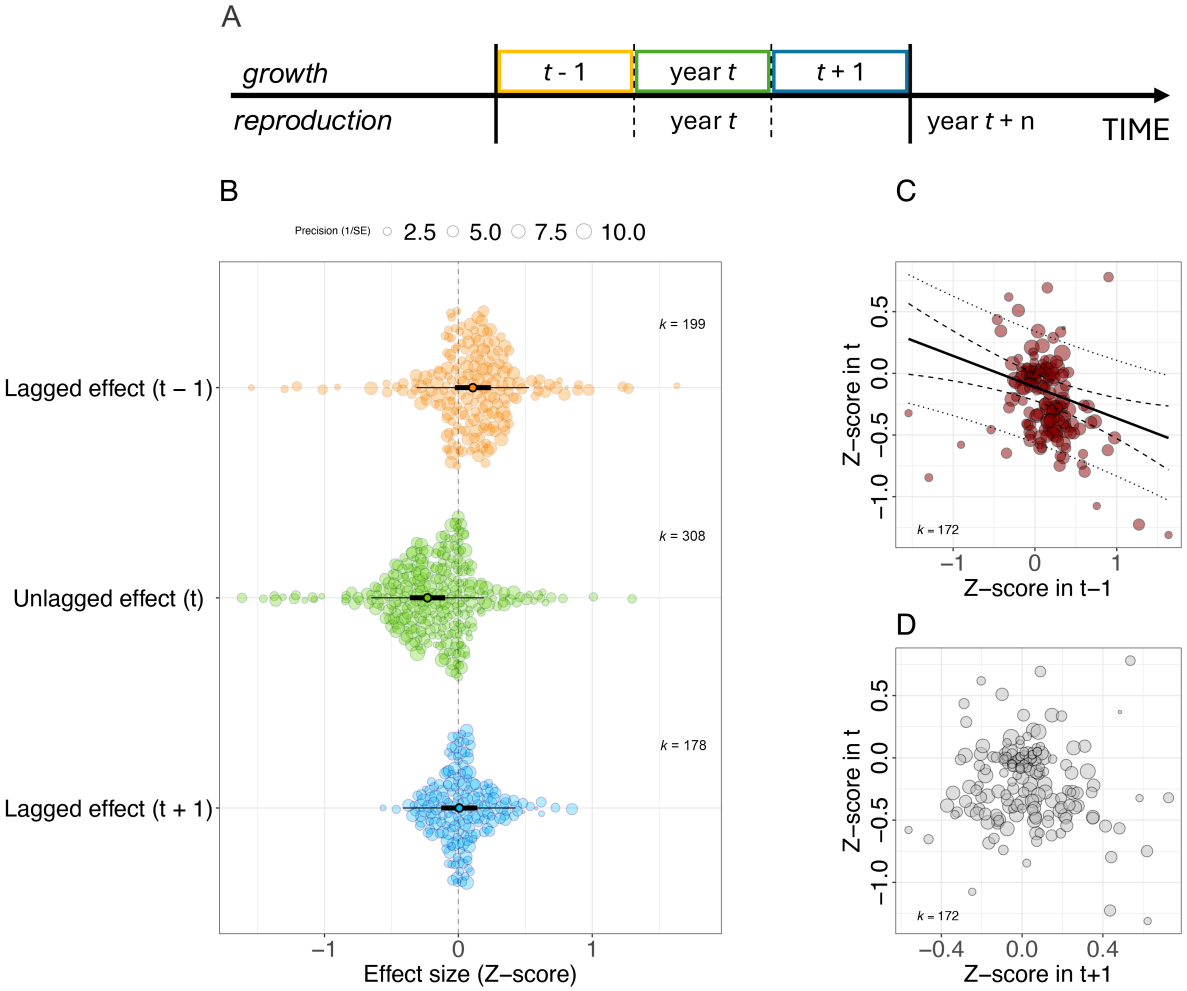


Figure 2: Growth is reduced in years of high seed production. (A) The temporal framework to study growth–reproduction correlations across multiple years, accounting for the within-year and lagged effect of growth ($t-1$, t, and $t+1$ in relation to reproduction in year t). (B) Relationships between reproduction and growth in the preceding year ($t-1$), same year (t), and the subsequent year ($t+1$). Black points show estimated effect sizes with 95% confidence intervals (CI; thicker bars) and 95% prediction intervals (PI; thinner bars). The relationship between the growth-reproduction correlation (Z-score) in the same year (t) and C) the growth-reproduction correlation in the preceding year ($t-1$), and D) the growth-reproduction correlation in the following year ($t+1$). Line at C) shows the relationship as estimated with phylogenetically informed multilevel meta-analytic model, associated 95% confidence intervals (dashed line), and 95% prediction intervals (dotted line). Points represent population-level effect sizes (k), with point size proportional to their precision (inverse SE). Model summary provided in Table S6 for B and Table S8 for C and D.

oaks, for example, *Quercus robur* had a positive effect size on average, while *Q. suber* or *Q. velutina* negative. Similarly, the negative effect sizes in *Fagus sylvatica* and *F. crenata*, contrasted with near-zero correlation in *F. grandifolia*. Closely related *Pinus nigra* and *P. sylvestris* were characterized by negative and positive effect sizes, respectively.

For comparison, we also evaluated phylogenetic signal in the functional traits represented in our dataset (Table S5). Pagel's λ (lambda) indicated strong phylogenetic structure in seed mass, SLA, and plant height, and moderate structure in wood density. Blomberg's K was low for all four traits (K = 0.009–0.054), although the signal was statistically significant for seed mass, wood density, and plant height. We note that these trait estimates are descriptive comparisons and do not establish that phylogenetic signal in growth–reproduction correlations can be reliably estimated from this species sample.

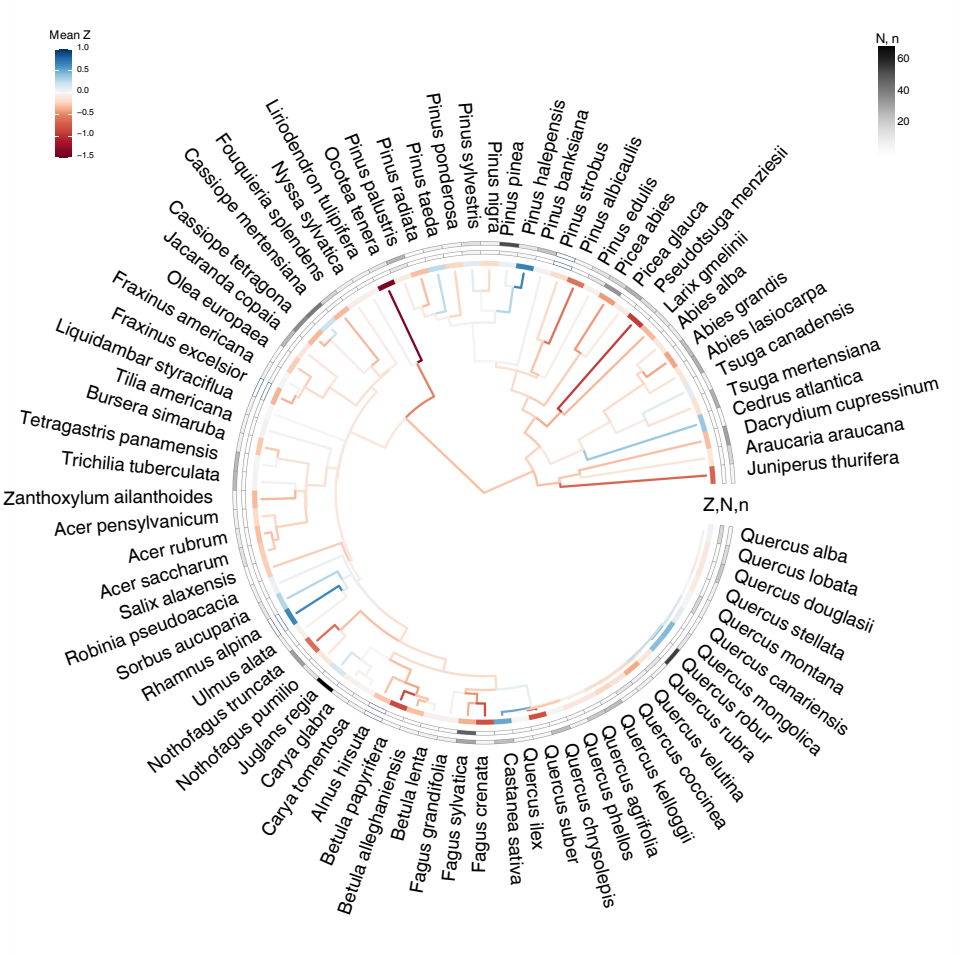


Figure 3: Growth–reproduction correlations across the sampled phylogeny. Red indicates negative, and blue indicates positive correlations between reproduction and growth in the same year (t). Phylogenetic signal, estimated from species-level mean effect sizes, is negligible (Pagel's $\lambda < 0.001$, $p = 1$, Blomberg's K = 0.016, $p = 0.004$, $n_{species} = 79$). The inner ring indicates the averaged Z values, whereas the gray-scale circles indicate sampling intensity, with shade proportional to the number of populations sampled (central ring, N) and mean number of years per species (outer ring, n) for each species (for the exact numbers see Fig. S4).

While we expected the negative correlation between growth and reproduction to be weaker in warm-moist sites, the interaction between mean annual temperature (MAT) and mean annual

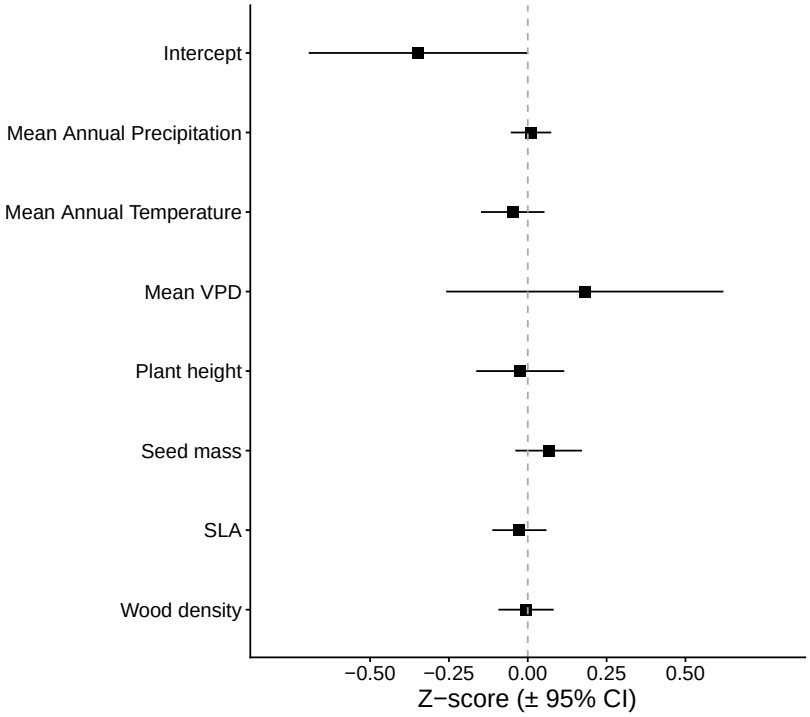


Figure 4: Growth–reproduction correlation shows no associations with climate or functional traits. Effect sizes and their 95% confidence intervals are derived from a phylogenetically informed multilevel comparative model ($n_{observations}$ = 308, $n_{species}$ = 79), with sampling variance incorporated at the observation level. All predictors were centered and scaled to facilitate direct comparison of effect sizes. Model summary provided in Table S10.

precipitation (MAP) was not significant (estimate = -0.019, p = 0.33). The trade-off did not vary systematically across sites differing in MAT (p = 0.36), MAP (p = 0.76), or mean VPD (p = 0.42) (Fig. 4, Table S10).

Wood density (p = 0.9) and specific leaf area (SLA, p = 0.54), two key traits reflecting the fast-slow continuum, were not significantly related to the trade-off between growth and reproduction (Fig. 4, Table S10). Likewise, the maximum height, which is reflecting the stature-recruitment trade-off, was not associated with the trade-off between growth and reproduction (p = 0.74, Fig. 4, Table S10). Finally, seed size, the key trait related to plant reproduction, was not associated with the trade-off between growth and reproduction (p = 0.22, Fig. 4, Table S10, see also Fig. S9 for bivariate relationships between Z-scores and climate/trait variables). The outcomes were consistent in both models regardless of the phylogeny supplied (Table S10, Table S11).

The correlations between growth and reproduction became weaker over time, especially for species with high interannual variation in reproduction (year × CV_p interaction: β = 0.021, p = 0.001, n = 261) (Fig. 5, Table S12). For example, in a species with an intermediate CV_p = 1, the estimated correlation between growth and reproduction was -0.16 in both 1980 and 2020. In contrast, in a species characterized by higher interannual variation in reproduction (CV_p = 1.6), the estimated correlation declined more than 7-fold over the 40 years, from -0.56 in 1980 to -0.08 in 2020 (Fig. 5B).

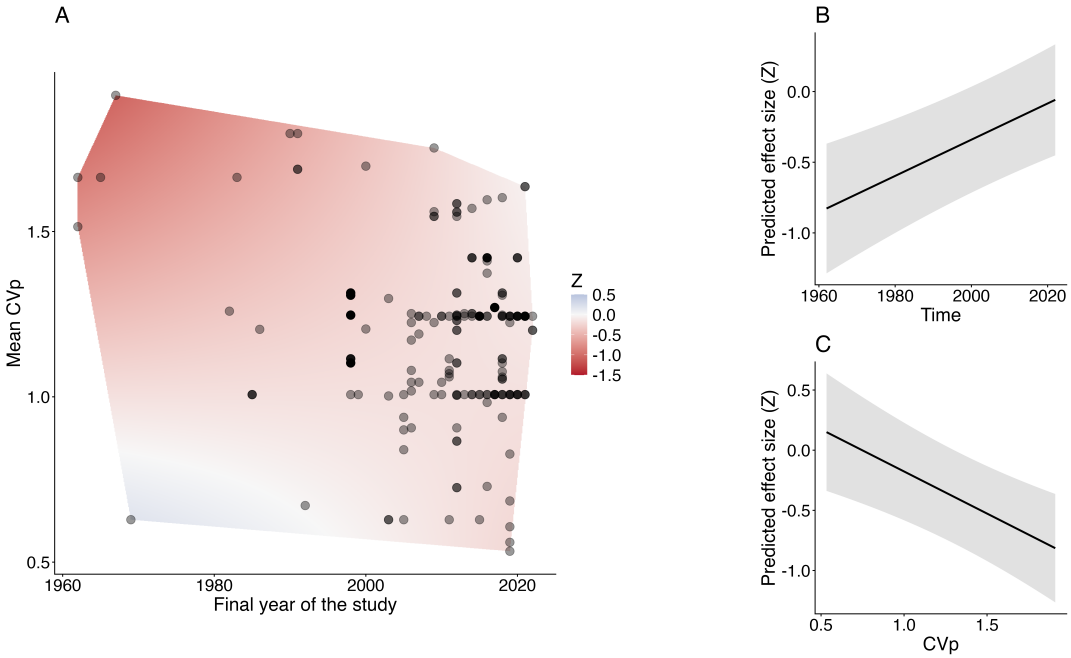


Figure 5: Negative growth–reproduction correlations weaken over time in strongly masting species. The surface plot at A) shows the estimated (unlagged) growth–reproduction correlation across combinations of population-level interannual variation in seed production (CV_p) and the final monitoring year of the study from which each effect size was extracted. Black dots denote data points that define the convex hull of the prediction space ($n_{populations}$ = 261, $n_{species}$ = 48). B) Temporal weakening of negative correlation between growth and reproduction, as estimated for CV_p = 1.6. C) The negative correlation between growth and reproduction is stronger in species characterized by higher CV_p, as estimated for year 1980. All predictions are derived from phylogenetically informed multilevel meta-analytic model, summarized in Table S12.

At the same time, in earlier decades of the dataset, species with high CV_p in seed production exhibited stronger negative growth–reproduction correlations than species with low CV_p (Fig. 5C). For example, in species with high reproductive variability (CV_p = 1.6), the estimated correlation was -0.56, whereas in species with relatively regular reproduction (CV_p = 0.6) the corresponding estimate was 0.12. Over time, however, growth–reproduction correlations converged across levels of reproductive variability. The sensitivity model based on the synthetic phylogenetic tree yielded similar output compared to the main model using the time-calibrated phylogeny (Table S12 , Table S13).

The year × CVp interaction was robust to the exclusion of individual taxa. It remained positive and statistically significant in all 48 models excluding one species at a time and all 16 models excluding one genus at a time, with similar effect-size estimates across the refitted models (Fig. S10).

Discussion

Our meta analysis indicates a trade-off between growth and reproduction in woody plants: growth and seed production are negatively correlated within the same year. In addition, the temporal structure of these correlations reveals asymmetric carry-over effects across years, consistent with delayed costs of reproduction expressed as constrained growth following high reproductive investment. Given limited species sampling, the low λ and K estimates do not support firm conclusions about phylogenetic signal. Neither spatial variation in climate nor functional traits systematically explained variation in effect sizes, suggesting that species resolve allocation conflicts in ways that are not tightly linked to biome, climatic regime, or ecological strategy. Notably, the trade-off was strongest in species with high interannual variability in reproduction but diminished over recent decades in these species, suggesting that changing resource dynamics under warming are reshaping the balance between growth and reproduction (Hacket-Pain *et al.*, 2025; Macias & Redmond, 2025). Our results indicate that while growth–reproduction trade-offs are widespread, their expression is flexible and responsive to contemporary environmental change (summarized in Table 1).

Within-year trade-offs dominated growth-reproduction dynamics, but lagged correlations revealed a pronounced asymmetry around reproductive events. Growth and seed production were negatively correlated in the same year. Growth in year $t-1$ was positively associated with reproduction in year t, although statistical support for this association depended on the phylogeny used. Nevertheless, the association between preceding-year and within-year effect sizes was strongest in populations with stronger within-year growth suppression. This pattern indicates that the pre-reproductive growth signal primarily reflects large contrasts between years when growth is strongly suppressed by reproductive investment and preceding years when reproduction is minimal (Koenig *et al.*, 2003; Foest *et al.*, 2025). In contrast, reproduction in year t was not associated with growth in year $t+1$. Given the temporal autocorrelation of reproduction, the absence of elevated growth in the post-reproductive year contrasts with the expectation of low reproductive investment and indicates constrained growth following reproduction. These results support resource-budget models in which reproduction draws on resources accumulated in previous years and replenishment after mast events competes with growth, such that delayed costs are expressed as asymmetric temporal patterns around reproductive events rather than as a consistent lagged reduction in growth (Satake & Iwasa, 2000; Han *et al.*, 2017; Kelly *et al.*, 2025). This interpretation, by adjusting the null expectation to account for the autocorrelation in reproduction, contrasts with earlier interpretations of positive growth anomalies at $t-1$ indicating resource accumulation, or a lack of growth response at $t+1$ as indicating an absence of delayed costs of reproduction (Hacket-Pain *et al.*, 2017; Drobyshev *et al.*, 2010; Nussbaumer *et al.*, 2021).

Reproductive traits such as seed size, fruit type, and interannual variability in seed production are often phylogenetically conserved (Moles *et al.*, 2005; Wang *et al.*, 2022; Journé *et al.*, 2023).

Table 1: Summary of results across hypotheses. Hypotheses are stated in shortened form; results summarize the direction and support in the meta-analysis.

Hypothesis	**Result summary**
Within-year allocation trade-off	Growth and reproduction are negatively correlated within the same year, indicating a widespread immediate cost of reproduction.
Lagged costs of reproduction	Growth tended to be higher in the year before reproduction, although statistical support depended on the phylogeny used; growth was not elevated after reproduction, consistent with delayed post-reproductive growth constraints.
Phylogenetic constraint	Closely related species differ strongly in trade-off strength and sign. Note that the sample does not permit reliable assessment or bounding of phylogenetic signal in growth–reproduction correlations;
Trait mediation	Functional traits (wood density, SLA, height, seed mass) do not explain variation in trade-off strength.
Climatic modulation	Trade-off strength is not systematically related to mean annual temperature, precipitation and VPD across sites.
Reproductive variability (CV_p)	Species with high interannual reproductive variability exhibit stronger negative growth–reproduction correlations.
Temporal change	Negative growth–reproduction correlations weaken over recent decades, particularly in species with high reproductive variability.

Within our dataset, growth-reproduction correlations varied markedly among sampled species, with positive and negative values occurring within *Quercus*, *Fagus*, *Pinus*, and *Tsuga*. Given the limited and uneven taxonomic sampling, firm conclusions about phylogenetic signal cannot be drawn. Broader and more balanced taxon sampling could reveal phylogenetic structure, or lack of it, that the present dataset cannot resolve. Phylogenetic effects may also be scale-dependent, with conservatism across deeper branches but greater lability within recent ecological radiations, such as oaks. Distinguishing these possibilities will require denser sampling within and among lineages.

We also found no evidence that spatial variation in climate modulates the trade-off. Neither mean annual temperature, mean annual precipitation, vapor pressure deficit, nor their interaction predicted variation in the growth–reproduction correlation. This result contrasts with the expectation that warm–moist sites should weaken trade-offs by easing resource limitation, while hot–dry climates should strengthen them. Several mechanisms may explain this mismatch. First, these site-level climatic variables test for spatial differences among populations, rather than whether the trade-off changes among years within populations. Within-season water stress and extreme events may nevertheless drive resource limitation or sink activity (Espelta *et al.*, 2008; Körner *et al.*, 2023; Cabon, 2025), but their effects on annual growth–reproduction relationships cannot be resolved from correlations summarized across multiple years and are therefore beyond the scope of our meta-analytic model. Second, growth and reproduction may respond in parallel to local climate, so that their correlation is conserved even when absolute rates change (Locosselli *et al.*, 2020; Ward *et al.*, 2025). Third, local edaphic variation and stand structure can buffer or amplify climatic effects (Barringer *et al.*, 2013), reducing the signal of broad-scale climate drivers in meta-analytic models.

Similarly, functional traits associated with the fast–slow continuum and the stature–recruitment axis did not show associations with the growth–reproduction correlation. Wood density, specific leaf area, maximum height, and seed size were all poor predictors of trade-off strength. This suggests that simple trait syndromes, while powerful for predicting demographic rates and fecundity (Rüger *et al.*, 2018; Qiu *et al.*, 2022; Bogdziewicz *et al.*, 2023), may not map directly to how plants partition resources between growth and reproduction from year to year, especially under variable environmental conditions (Augusto *et al.*, 2025). In fact, a recent global analysis failed to detect the expected links between acquisitive trait syndromes and high growth rates in natural forests, as environmental constraints override trait-based growth potential across species (Augusto *et al.*, 2025). Trade-offs may instead be governed by unmeasured axes of variation, such as non-structural carbohydrate storage dynamics (Trugman & Anderegg, 2025) or phenological strategies (Journé *et al.*, 2021; Etzold *et al.*, 2021; Wolkovich *et al.*, 2025), which are rarely quantified across many species but may determine how plants buffer or transmit resource limitations into growth and seed output.

The temporal trend in our dataset reveals that in strongly masting species, the negative growth–reproduction correlation has weakened over recent decades. First, the strong relationship

between the interannual variation in reproduction (CV_p) and growth–reproduction trade-off supports an early, but so far untested, prediction that high variation in reproductive allocation in strongly masting species should render the detection of costs of reproduction more likely in such species (Norton & Kelly, 1988). The weakening of the trade-off over time aligns with the long-term evidence from European beech and Japanese oak (*Quercus crispula*), in which warming increased the frequency of weather cues that trigger reproduction, leading to more frequent seed crops, and in the case of beech, reserve depletion, and an erosion of the growth–reproduction trade-off (Foest *et al.*, 2024; Hacket-Pain *et al.*, 2025; Shibata *et al.*, 2020). Our results indicate that this weakening of the growth–reproduction trade-off is not unique to beech, implying a more general disruption of how trees balance competing demands on limited resources. Such disruption matters because growth–reproduction correlations reflect underlying resource allocation processes. Warming can push these processes out of balance, with consequences that extend from growth and reproduction to survival, defense, and overall resilience (Lauder *et al.*, 2019; Macias & Redmond, 2025). A weakening trade-off therefore does not necessarily signal relaxed resource limitation. Rather, it may indicate that trees are increasingly unable to convert the opportunity for compensatory growth in years of reduced reproductive investment because reserves are depleted or physiological stress constrains recovery (Hacket-Pain *et al.*, 2025). In strongly masting species, this creates conditions where reproduction remains frequent while growth declines — a combination shown to reduce carbon storage, diminish future reproductive potential, and increase mortality (Qiu *et al.*, 2021; Hacket-Pain *et al.*, 2025; Bordin *et al.*, 2025). These temporal shifts suggest that climate change is altering the resource dynamics that underpin masting, weakening a fundamental component of demographic regulation in many forest trees.

We note that the temporal pattern was robust to the sequential exclusion of individual species and genera, indicating that it was not driven by any single taxon represented primarily during a particular part of the study period. Nevertheless, because species were unevenly represented through time, this analysis cannot fully separate temporal change from broader changes in species composition, and the pattern should be interpreted accordingly (see also Fig. S11).

Our findings come with several limitations. Although the database covers a broad geographic range, its taxonomic and geographic sampling is non-random. Sampling is concentrated in temperate and boreal regions, particularly in Europe and North America, with some lineages, including oaks and pines, disproportionately represented and many tropical and other woody lineages absent. While allocation strategies and environmental constraints may differ under such conditions, community-level studies suggest reduced growth during general flowering events in tropical Dipterocarp forests (Nakagawa *et al.*, 2012). Similarly, a larger species sample with broader trait and climate coverage could reveal patterns that were not detected here, despite the reasonable trait coverage of our dataset (Fig. S12). Measures of growth and reproduction also vary across studies—ranging from basal area increment and ring width to fruit counts and seed traps—introducing methodological heterogeneity that our models only partly capture (Fig. S3, Table S2, Table S3). Potentially important sources of variation, such as ontogenetic stage

(Thomas, 2011), stand age (Genet *et al.*, 2009; Ward *et al.*, 2025), or competitive environment (Clark *et al.*, 2014; Augusto *et al.*, 2025), were often unreported and could not be incorporated despite their possible influence on allocation patterns. Our analysis also largely focuses on secondary growth of the main stem, whereas primary growth may be more directly affected by reproductive investment, especially given the partial resource autonomy of branches (Hoch, 2005; Han *et al.*, 2011). Negative growth–reproduction relationships may also arise not from direct competition for shared resources but from independent sink limitation by external drivers — for example, weather conditions that favor reproduction while suppressing growth (Knops *et al.*, 2007; Mund *et al.*, 2020). Growth can also be actively down-regulated in years with high reproductive investment to maintain storage (Dietze *et al.*, 2014; Trugman & Anderegg, 2025). While such mechanisms could contribute to the patterns we detect, the meta-analysis was not designed to disentangle them. A further limitation is that most studies rely on among-year correlations averaged across individuals, even though trade-offs evolve and operate at the level of individual plants (Cople *et al.*, 2021). Many estimates of trade-offs therefore reflect aggregated data on growth and reproduction from different trees; if resource allocation depends strongly on individual-level resource acquisition, such aggregation could obscure or inflate underlying relationships. Finally, the 'decline effect' in meta-analyses, caused by an increasing tendency to publish null results (Nakagawa *et al.*, 2022), may overestimate temporal effects on trade-offs caused by a changing climate. Together, these limitations highlight the need for long-term datasets that jointly track individuals, multiple tissues, demographic stages, and environmental covariates to fully resolve how growth–reproduction relationships operate across species and biomes.

Taken together, our results show that growth–reproduction trade-offs are common among the woody species represented here, but show limited associations with the climatic and functional traits examined. The consistent same-year cost of reproduction, combined with asymmetric lagged effects in which high reproductive investment is followed by reduced growth, supports a resource-budget view in which allocation conflicts are expressed within years and lagged costs emerge following high reproductive investment (Satake & Iwasa, 2000; Koenig *et al.*, 2003). The limited climatic and trait associations suggest that trade-off strength also reflects local conditions and species-specific resource dynamics (Hacket-Pain *et al.*, 2017). The temporal weakening of the trade-off in high-CV_p species links these dynamics to climate change, suggesting that more frequent cueing and altered reserve trajectories can decouple growth responses from annual reproductive effort (Hacket-Pain *et al.*, 2025). Our meta-analysis calls for further research on resource-based individual-level quality of phenotypic correlations between growth and reproduction in woody plants in relation to the changing climate.

Acknowledgements

We would like to acknowledge researchers who kindly shared their data: Sabine Braun, Simon Tresch, Sven Hopf, Angelika Kölbl, Burkhard Beudert, Bruno Fady, Maxime Cailleret, Manuel Esteban Lucas Borja, and Walt Koenig. This study was funded by the European Union (ERC, ForestFuture, 101039066; EC, FECUND, 101244227). Views and opinions expressed are however those of the authors only and do not necessarily reflect those of the European Union or the European Research Council. Neither the European Union nor the granting authority can be held responsible for them. JJF was also supported by the Foundation for Polish Science (FNP).

Competing interests

Authors have no competing interests to declare.

Author contributions

MKB, MB and AH-P conceived the study idea and developed research questions. MKB, MB, UE, MaB, VJ, KK, JS and AH-P performed the abstract screening. MKB extracted data from the literature and curated data. MKB led the analysis with the input from SMD, MB, VJ, JJF and JS. MKB wrote the first draft of the manuscript with substantial help from MB and AH-P. All authors contributed to the interpretation of the analysis, revised the draft, and gave their final approval for publication.

Data availability

The data and code supporting the results are available at https://github.com/maciejkbarczyk/Growth-reproduction_trade-offs_meta.

References

Abatzoglou, J.T., Dobrowski, S.Z., Parks, S.A. & Hegewisch, K.C. (2018). Terraclimate, a high-resolution global dataset of monthly climate and climatic water balance from 1958–2015. *Scientific Data*, 170191.

Adier, P.B., Salguero-Gómez, R., Compagnoni, A., Hsu, J.S., Ray-Mukherjee, J., Mbeau-Ache, C. *et al.* (2014). Functional traits explain variation in plant lifehistory strategies. *Proceedings of the National Academy of Sciences of the United States of America*, 111, 740–745.

Alfaro-Sánchez, R., Camarero, J.J., López-Serrano, F.R., Sánchez-Salguero, R., Moya, D. & De Las Hera, J. (2015). Positive coupling between growth and reproduction in young post-fire Aleppo pines depends on climate and site conditions. *International Journal of Wildland Fire*, 24, 507–517.

Augusto, L., Borelle, R., Boča, A., Bon, L., Charru, M. *et al.* (2025). Widespread slow growth of acquisitive tree species. *Nature*, 640, 395–401.

Barringer, B.C., Koenig, W.D. & Knops, J.M. (2013). Interrelationships among life-history traits in three california oaks. *Oecologia*, 171, 129–139.

Bogdziewicz, M., Acuña, M.C.A., Andrus, R., Ascoli, D., Bergeron, Y., Brveiller, D. *et al.* (2023). Linking seed size and number to trait syndromes in trees. *Global Ecology and Biogeography*, 32, 683–694.

Bogdziewicz, M., Crone, E., Steele, M. & Zwolak, R. (2017). Effects of nitrogen deposition on reproduction in a masting tree: benefits of higher seed production are trumped by negative biotic interactions. *Journal of Ecology*, 105, 310–320.

Bogdziewicz, M., Fernández-Martínez, M., Espelta, J.M., Ogaya, R. & Penuelas, J. (2020). Is forest fecundity resistant to drought? Results from an 18-yr rainfall-reduction experiment. *New Phytologist*, 227, 1073–1080.

Bogdziewicz, M., Kelly, D., Ascoli, D., Caignard, T., Chianucci, F., Crone, E.E. *et al.* (2024). Evolutionary ecology of masting: mechanisms, models, and climate change. *Trends in Ecology & Evolution*, 39, 851–862.

Bordin, K.M., Bauman, D., Pugh, T.A., Müller, S.C., Phillips, O.L., Fortunel, C. *et al.* (2025). Growth–survival trade-off in temperate trees is weak and restricted to late-successional stages. *Journal of Ecology*, 113, 3466–3477.

Braun, S., Schindler, C. & Rihm, B. (2017). Growth trends of beech and Norway spruce in Switzerland: The role of nitrogen deposition, ozone, mineral nutrition and climate. *Science of the Total Environment*, 599, 637–646.

Brown, M.J.M., Walker, B.E., Black, N., Govaerts, R.H.A., Ondo, I., Turner, R. *et al.* (2023). rWCVP: a companion R package for the World Checklist of Vascular Plants. *New Phytologist*, 240, 1355–1365.

Cabon, A. (2025). Distal to proximal: a continuum of drivers shaping tree growth and carbon partitioning. *New Phytologist*, 249, 729–735.

Chave, J., Coomes, D., Jansen, S., Lewis, S.L., Swenson, N.G. & Zanne, A.E. (2009). Towards a worldwide wood economics spectrum. *Ecology Letters*, 12, 351–366.

Clark, J.S., Andrus, R., Aubry-Kientz, M., Bergeron, Y., Bogdziewicz, M., Bragg, D.C. *et al.* (2021). Continent-wide tree fecundity driven by indirect climate effects. *Nature Communications*, 12, 1–11.

Clark, J.S., Bell, D.M., Kwit, M.C. & Zhu, K. (2014). Competition-interaction landscapes for the joint response of forests to climate change. *Global Change Biology*, 20, 1979–1991.

Cople, O., Keefover-Ring, K., Kruger, E.L. & Lindroth, R.L. (2021). Growth–defense tradeoffs shape population genetic composition in an iconic forest tree species. *PNAS*, 118, e2103162118.

Dietze, M.C., Sala, A., Carbone, M.S., Czimczik, C.I., Mantooth, J.A., Richardson, A.D. *et al.* (2014). Nonstructural carbon in woody plants. *Annual Review of Plant Biology*, 65, 667–687.

Dohrenbusch, A., Jaehne, S., Bredemeier, M. & Lamersdorf, N. (2002). Growth and fructification of a Norway spruce (*Picea abies* L. Karst) forest ecosystem under changed nutrient and water input. *Annals of Forest Science*, 59, 359–368.

Dorken, M.E., van Kleunen, M. & Stift, M. (2025). Costs of reproduction in flowering plants. *New Phytologist*, 147, 55–70.

Drobyshev, I., Övergaard, R., Saygin, I., Niklasson, M., Hickler, T., Karlsson, M. *et al.* (2010). Masting behaviour and dendrochronology of European beech (*Fagus sylvatica* L.) in southern sweden. *Forest Ecology and Management*, 259, 2160–2171.

Díaz, S., Kattge, J., Cornelissen, J.H., Wright, I.J., Lavorel, S., Dray, S. *et al.* (2016). The global spectrum of plant form and function. *Nature*, 529, 167–171.

Espelta, J.M., Cortés, P., Molowny-Horas, R., Sánchez-Humanes, B. & Retana, J. (2008). Masting mediated by summer drought reduces acorn predation in mediterranean oak forests. *Ecology*, 89, 805–817.

Esquivel-Muelbert, A., Banbury Morgan, R., Brienen, R., Gloor, E., Lewis, S.L., Dexter, K.G. *et al.* (2025). Increasing tree size across Amazonia. *Nature Plants*, 11, 2016–2025.

Etzold, S., Ferretti, M., Reinds, G.J., Solberg, S., Gessler, A., Waldner, P. *et al.* (2020). Nitrogen deposition is the most important environmental driver of growth of pure, even-aged and managed European forests. *Forest Ecology and Management*, 458, 117762.

Etzold, S., Sterck, F., Bose, A.K., Braun, S., Buchmann, N., Eugster, W. *et al.* (2021). Number of growth days and not length of the growth period determines radial stem growth of temperate trees. *Ecology Letters*, 25, 427–439.

Fick, S.E. & Hijmans, R.J. (2017). WorldClim 2: new 1-km spatial resolution climate surfaces for global land areas. *International Journal of Climatology*, 37, 4302–4315.

Foest, J.J., Bogdziewicz, M., Pesendorfer, M.B., Ascoli, D., Cutini, A., Nussbaumer, A. *et al.* (2024). Widespread breakdown in masting in European beech due to rising summer temperatures. *Global Change Biology*, 30, e17307.

Foest, J.J., Caignard, T., Pearse, I.S., Bogdziewicz, M. & Hacket-Pain, A. (2025). Intraspecific variation in masting across climate gradients is inconsistent with the environmental stress hypothesis. *Ecology*, 106, e70076.

Garcia-Barreda, S., Sangüesa-Barreda, G., Madrigal-González, J., Seijo, F., González de Andrés, E. & Camarero, J.J. (2021). Reproductive phenology determines the linkages between radial growth, fruit production and climate in four Mediterranean tree species. *Agricultural and Forest Meteorology*, 307, 108493.

Genet, H., Bréda, N. & Dufrêne, E. (2009). Age-related variation in carbon allocation at tree and stand scales in beech (*Fagus sylvatica* L.) and sessile oak sessile oak (*Quercus petraea* (Matt.) Liebl.) using a chronosequence approach. *Tree Physiology*, 30, 177–192.

Hacket-Pain, A. & Bogdziewicz, M. (2021). Climate change and plant reproduction: trends and drivers of mast seeding change. *Philosophical Transactions of the Royal Society B*, 376, 20200379.

Hacket-Pain, A., Foest, J.J., Pearse, I.S., LaMontagne, J.M., Koenig, W.D., Vacchiano, G. *et al.* (2022). Mastree+: Time-series of plant reproductive effort from six continents. *Global Change Biology*, 28, 3066–3082.

Hacket-Pain, A., Szymkowiak, J., Journé, V., Barczyk, M.K., Thomas, P.A., Lageard, J.G.A. *et al.* (2025). Growth decline in European beech associated with temperature-driven increase in reproductive allocation. *Proceedings of the National Academy of Sciences*, 122, e2423181122.

Hacket-Pain, A.J., Ascoli, D., Vacchiano, G., Biondi, F., Cavin, L., Conedera, M. *et al.* (2018). Climatically controlled reproduction drives interannual growth variability in a temperate tree species. *Ecology Letters*, 21, 1833–1844.

675 Hacket-Pain, A.J., Lageard, J.G. & Thomas, P.A. (2017). Drought and reproductive effort
676 interact to control growth of a temperate broadleaved tree species (*Fagus sylvatica*). *Tree*
677 *Physiology*, 37, 744–754.

678 Hadad, M.A., Roig, F.A., Molina, J.G.A. & Hacket-Pain, A. (2021). Growth of male and female
679 *Araucaria araucana* trees respond differently to regional mast events, creating sex-specific
680 patterns in their tree-ring chronologies. *Ecological Indicators*, 122, 107245.

681 Han, Q., Kabeya, D. & Hoch, G. (2011). Leaf traits, shoot growth and seed production in mature
682 *Fagus sylvatica* trees after 8 years of CO2 enrichment. *Annals of Botany*, 107, 1405–1411.

683 Han, Q., Kabeya, D. & Inagaki, Y. (2017). Influence of reproduction on nitrogen uptake and
684 allocation to new organs in *Fagus crenata*. *Tree Physiology*, 37, 1436–1443.

685 Hesse, B.D., Hartmann, H., Rötzer, T., Landhäusser, S.M., Goisser, M., Weikl, F. *et al.* (2021).
686 Mature beech and spruce trees under drought – Higher C investment in reproduction at the
687 expense of whole-tree NSC stores. *Environmental and Experimental Botany*, 191, 104615.

688 Hoch, G. (2005). Fruit-bearing branchlets are carbon autonomous in mature broad-leaved
689 temperate forest trees. *Plant, Cell and Environment*, 28, 651–659.

690 Hulshof, C.M., Stegen, J.C., Swenson, N.G., Enquist, C.A.F. & Enquist, B.J. (2012). Interannual
691 variability of growth and reproduction in *Bursera simaruba*: the role of allometry and resource
692 variability. *Ecology*, 93, 180–190.

693 Isagi, Y., Sugimura, K., Ssumida, A. & Ito, H. (1997). How does masting happen and synchro-
694 nize? *Journal of Theoretical Biology*, 187, 231–239.

695 Jablonski, L.M., Wang, X. & Curtis, P.S. (2002). Plant reproduction under elevated CO2
696 conditions: a meta-analysis of reports on 79 crop and wild species. 156, 9–26.

697 Journé, V., Andrus, R., Aravena, M.C., Ascoli, D., Berretti, R., Berveiller, D. *et al.* (2022).
698 Globally, tree fecundity exceeds productivity gradients. *Ecology Letters*, 25, 1471–1482.

699 Journé, V., Caignard, T., Hacket-Pain, A. & Bogdziewicz, M. (2021). Leaf phenology correlates
700 with fruit production in European beech (*Fagus sylvatica*) and in temperate oaks (*Quercus*
701 *robur* and *Quercus petraea*). *European Journal of Forest Research*, 140, 733–744.

702 Journé, V., Hacket-Pain, A. & Bogdziewicz, M. (2023). Evolution of masting in plants is linked
703 to investment in low tissue mortality. *Nature Communications*, 14, 7998.

704 Kabeya, D., Iio, A., Kakubari, Y. & Han, Q. (2021). Dynamics of non-structural carbohydrates
705 following a full masting event reveal a role for stored starch in relation to reproduction in
706 *Fagus crenata*. *Forestry Research*, 1, 18.

Kabeya, D., Inagaki, Y., Noguchi, K. & Han, Q. (2017). Growth rate reduction causes a decline in the annual incremental trunk growth in masting *Fagus crenata* trees. *Tree Physiology*, 37, 1444–1452.

Kambach, S., Condit, R., Aguilar, S., Bruelheide, H., Bunyavejchewin, S., Chang-Yang, C.H. *et al.* (2022). Consistency of demographic trade-offs across 13 (sub)tropical forests. *Journal of Ecology*, 10, 35.

Kattge, J., Bönisch, G., Díaz, S., Lavorel, S., Prentice, I.C., Leadley, P. *et al.* (2020). Try plant trait database – enhanced coverage and open access. *Global Change Biology*, 26, 119–188.

Kelly, D., Szymkowiak, J., Hacket-Pain, A. & Bogdziewicz, M. (2025). Fine-tuning mast seeding: as resources accumulate, plants become more sensitive to weather cues. *New Phytologist*, 246, 1975–1985.

Klesse, S., Peters, R., Alfaro-Sánchez, R., Badeau, V., Baittinger, C., Battipaglia, G. *et al.* (2024). No future growth enhancement expected at the northern edge for European beech due to continued water limitation. *Global Change Biology*, 30, e17546.

Knops, J.M.H., Koenig, W.D. & Carmen, W.J. (2007). Negative correlation does not imply a tradeoff between growth and reproduction in California oaks. *Proceedings of the National Academy of Sciences*, 104, 16982–16985.

Koenig, W.D., Kelly, D., Sork, V.L., Duncan, R.P., Elkinton, J.S., Peltonen, M.S. *et al.* (2003). Dissecting components of population-level variation in seed production and the evolution of masting behavior. *Oikos*, 102, 581–591.

Körner, C., Möhl, P. & Hiltbrunner, E. (2023). Four ways to define the growing season. *Ecology Letters*, 26, 1277–1292.

Lauder, J.D., Moran, E.V. & Hart, S.C. (2019). Fight or flight? potential tradeoffs between drought defense and reproduction in conifers. *Tree Physiology*, 39, 1071–1085.

Locosselli, G.M., Brienen, J.W., Leite, M.D.S., Gloor, M., Krottenthaler, S., Oliveira, A.A.D. *et al.* (2020). Global tree-ring analysis reveals rapid decrease in tropical tree longevity with temperature. *PNAS*, 117, 33358–33364.

Macias, D.S. & Redmond, M.D. (2025). Climate-warming alters resource allocation in unpredictable ways. *Trends in Ecology and Evolution*, 40, 428–430.

Magill, A.H., Aber, J.D., Currie, W.S., Nadelhoffer, K.J., Martin, M.E., McDowell, W.H. *et al.* (2004). Ecosystem response to 15 years of chronic nitrogen additions at the Harvard Forest LTER, Massachusetts, USA. *Forest Ecology and Management*, 196, 7–28.

Michonneau, F., Brown, J.W. & Winter, D.J. (2016). rotl: an R package to interact with the Open Tree of Life data. *Methods in Ecology and Evolution*, 7, 1476–1481.

Mo, L., Crowther, T.W., Maynard, D.S., van den Hoogen, J., Ma, H., Bialic-Murphy, L. *et al.* (2024). The global distribution and drivers of wood density and their impact on forest carbon stocks. *Nature Ecology Evolution*, 8, 2195–2212.

Moles, A., Ackerly, D., Webb, C., Tweddle, J., Dickie, J. & Westboy, M. (2005). A brief history of seed size. *Science*, 307, 576–580.

Monks, A., Monks, J.M. & Tanentzap, A.J. (2016). Resource limitation underlying multiple masting models makes mast seeding sensitive to future climate change. *New Phytologist*, 210, 419–430.

Mund, M., Herbst, M., Knohl, A., Matthäus, B., Schumacher, J., Schall, P. *et al.* (2020). It is not just a 'trade-off': indications for sink- and source-limitation to vegetative and regenerative growth in an old-growth beech forest. *New Phytologist*, 226, 111–125.

Nakagawa, M., Matsushita, M., Kurokawa, H., Samejima, H., Takeuchi, Y., Aiba, M. *et al.* (2012). Possible negative effect of general flowering on tree growth and aboveground biomass increment in a bornean tropical rain forest. *Biotropica*, 44, 720–729.

Nakagawa, S., Lagisz, M., Jennions, M.D., Koricheva, J., Noble, D.W.A., Parker, T.H. *et al.* (2022). Methods for testing publication bias in ecological and evolutionary meta-analyses. *Methods in Ecology and Evolution*, 13, 4–21.

Nakagawa, S., Lagisz, M., O'Dea, R.E., Pottier, P., Rutkowska, J., Senior, A.M. *et al.* (2023). orchaRd 2.0: An R package for visualising meta-analyses with orchard plots. *Methods in Ecology and Evolution*, 14, 2003–2010.

Norby, R.J., Loader, N.J., Mayoral, C., Ullah, S., Curioni, G., Smith, A.R. *et al.* (2024). Enhanced woody biomass production in a mature temperate forest under elevated CO2. *Nature Climate Change*, 14, 983–988.

Norton, D.A. & Kelly, D. (1988). Mast seeding over 33 years by Dacrydium cupressinum Lamb. (rimu) (*Podocarpaceae*) in New Zealand: The importance of economies of scale. *Functional Ecology*, 2, 399–408.

Nussbaumer, A., Gessler, A., Benham, S., de Cinti, B., Etzold, S., Ingerslev, M. *et al.* (2021). Contrasting resource dynamics in mast years for European beech and oak—a continental scale analysis. *Frontiers in Forests and Global Change*, 4, 89.

Obeso, J.R. (2002). The costs of reproduction in plants. *New Phytologist*, 155, 321–348.

O'Dea, R., Lagisz, M., Jennions, M., Koricheva J.and Noble, D., Parker, T., Gurevitch, J. *et al.* (2021). Preferred reporting items for systematic reviews and meta-analyses in ecology and evolutionary biology: a prisma extension. *Biological Reviews*, 96, 1695–1722.

Paradis, E. & Schliep, K. (2019). ape 5.0: an environment for modern phylogenetics and evolutionary analyses in R. *Bioinformatics*, 35, 526–528.

Patterson, T.W., Greenberg, C.H. & Hacket-Pain, A. (2023). Acorn production, climate, and tree-ring growth of five oak species in southern Appalachian forests. *Forest Ecology and Management*, 546, 121310.

Pearse, I.S., Koenig, W.D. & Kelly, D. (2016). Mechanisms of mast seeding: resources, weather, cues, and selection. *New Phytologist*, 212, 546–562.

Pearse, I.S., LaMontagne, J.M., Lordon, M., Hipp, A.L. & Koenig, W.D. (2020). Biogeography and phylogeny of masting: do global patterns fit functional hypotheses? *New Phytologist*, 227, 1557–1567.

Perret, D.L., Evans, M.E. & Sax, D.F. (2024). A species' response to spatial climatic variation does not predict its response to climate change. *Proceedings of the National Academy of Sciences of the United States of America*, 121, e2304404120.

Pottier, P., Noble, D.W.A., Seebacher, F., Wu, N.C., Burke, S., Lagisz, M. *et al.* (2024). New horizons for comparative studies and meta-analyses. *Trends in Ecology & Evolution*, 39, 435–445.

Qiu, T., Andrus, R., Aravena, M.C., Ascoli, D., Bergeron, Y., Berretti, R. *et al.* (2022). Limits to reproduction and seed size-number trade-offs that shape forest dominance and future recovery. *Nature Communications*, 13, 1–12.

Qiu, T., Aravena, M.C., Andrus, R., Ascoli, D., Bergeron, Y., Berretti, R. *et al.* (2021). Is there tree senescence? The fecundity evidence. *Proceedings of the National Academy of Sciences of the United States of America*, 118, e2106130118.

Qiu, T., Aravena, M.C., Ascoli, D., Bergeron, Y., Bogdziewicz, M., Boivin, T. *et al.* (2023). Masting is uncommon in trees that depend on mutualist dispersers in the context of global climate and fertility gradients. *Nature Plants*, 9, 1044–1056.

R Core Team (2024). *R: A Language and Environment for Statistical Computing*. R Foundation for Statistical Computing, Vienna, Austria.

Reich, P.B. (2014). The world-wide 'fast-slow' plant economics spectrum: A traits manifesto. *Journal of Ecology*, 102, 275–301.

Rowland, L., da Costa, A.C., Oliveira, A.A., Almeida, S.S., Ferreira, L.V., Malhi, Y. *et al.* (2018). Shock and stabilisation following long-term drought in tropical forest from 15 years of litterfall dynamics. *Journal of Ecology*, 106, 1673–1682.

Russo, S.E., McMahon, S.M., Detto, M., Ledder, G., Wright, S.J., Condit, R.S. *et al.* (2020). The interspecific growth–mortality trade-off is not a general framework for tropical forest community structure. *Nature Ecology & Evolution*, 5, 174–183.

Rüger, N., Comita, L.S., Condit, R., Purves, D., Rosenbaum, B., Visser, M.D. *et al.* (2018). Beyond the fast–slow continuum: demographic dimensions structuring a tropical tree community. *Ecology Letters*, 21, 1075–1084.

Sala, A., Hopping, K., McIntire, E.J., Delzon, S. & Crone, E.E. (2012). Masting in whitebark pine (*Pinus albicaulis*) depletes stored nutrients. *New Phytologist*, 196, 189–199.

Satake, A. & Iwasa, Y. (2000). Pollen coupling of forest trees: Forming synchronized and periodic reproduction out of chaos. *Journal of Theoretical Biology*, 203, 63–84.

Sharma, S., Andrus, R., Bergeron, Y., Bogdziewicz, M., Bragg, D.C., Brockway, D. *et al.* (2022). North american tree migration paced by climate in the west, lagging in the east. *Proceedings of the National Academy of Sciences*, 119, e2116691118.

Shestakova, T.A., Mutke, S., Gordo, J., Camarero, J.J., Sin, E., Pemán, J. *et al.* (2021). Weather as main driver for masting and stem growth variation in stone pine supports compatible timber and nut co-production. *Agricultural and Forest Meteorology*, 298-299, 108287.

Shibata, M., Masaki, T., Yagihashi, T., Shimada, T. & Saitoh, T. (2020). Decadal changes in masting behaviour of oak trees with rising temperature. *Journal of Ecology*, 108, 1088–1100.

Stefan, V. & Levin, S. (2025). *plotbiomes: Plot Whittaker biomes with ggplot2*. R package version 0.0.0.9001.

Szymkowiak, J., Bogdziewicz, M., Kelly, D., Foest, J., Braun, S., Beudert, B. *et al.* (2026). European beech reproduction is not reduced by drought, including the 2003, 2018, and 2022 extremes. *Proceedings of the National Academy of Sciences*, 123, e2607167123.

Thomas, S.C. (2011). Age-related changes in tree growth and functional biology: The role of reproduction. In: *Size- and Age-Related Changes in Tree Structure and Function* (eds. Meinzer, F.C., Lachenbruch, B. & Dawson, T.E.). Springer, pp. 33–64.

Trugman, A.T. & Anderegg, L.D. (2025). Source vs sink limitations on tree growth: from physiological mechanisms to evolutionary constraints and terrestrial carbon cycle implications. *New Phytologist*, 245, 966–981.

Viechtbauer, W. (2010). Conducting meta-analyses in R with the metafor package. *Journal of Statistical Software*, 36, 1–48.

Violle, C., Navas, M.L., Vile, D., Kazakou, E., Fortunel, C., Hummel, I. *et al.* (2007). Let the concept of trait be functional! *Oikos*, 116, 882–892.

Wang, G., Ives, A.R., Zhu, H., Tan, Y., Chen, S.C., Yang, J. *et al.* (2022). Phylogenetic conservatism explains why plants are more likely to produce fleshy fruits in the tropics. *Ecology*, 103, e03555.

Ward, R.E., Zhang-Zheng, H., Abernethy, K., Adu-Bredu, S., Arroyo, L., Bailey, A. *et al.* (2025). Forest age rivals climate to explain reproductive allocation patterns in forest ecosystems globally. *Ecology Letters*, 28, e70191.

Williams, G.C. (1966). Natural selection, the costs of reproduction, and a refinement of lack's principle. *The American Naturalist*, 100, 687–690.

Wolkovich, E.M., Ettinger, A.K., Chin, A.R., Chamberlain, C.J., Baumgarten, F., Pradhan, K. *et al.* (2025). Why longer seasons with climate change may not increase tree growth. *Nature Climate Change*, 15, 1283–1292.

Woodward, A., Silsbee David, G., Schreiner Edward, G. & Means Joseph, E. (1994). Influence of climate on radial growth and cone production in subalpine fir (*Abies lasiocarpa*) and mountain hemlock (*Tsuga mertensiana*). *Canadian Journal of Forest Research*, 24, 1283–1292.

Zanne, A.E., Tank, D.C., Cornwell, W.K., Eastman, J.M., Smith, S.A., FitzJohn, R.G. *et al.* (2014). Three keys to the radiation of angiosperms into freezing environments. *Nature*, 506, 89–92.

Supporting Information

Tab. S1 Search summary.

Tab. S2 Summary of the primary rma model testing the growth-reproduction relationships in relation to the different data categories.

Tab. S3 Summary of the complementary rma model testing the growth-reproduction relationships in relation to the different data categories.

Tab. S4 Effect size formulas.

Tab. S5 Descriptive estimates of Pagel's lambda and Blomberg's K for functional traits in the sampled species.

Tab. S6 Estimated mean growth–reproduction correlations across three temporal alignments in the primary meta-analytic model.

Tab. S7 Estimated mean growth–reproduction correlations across three temporal alignments in the complementary meta-analytic model.

Tab. S8 Summary of the primary rma model testing the relationships between the within-population growth–reproduction correlations.

Tab. S9 Summary of the complementary rma model testing the relationships between the within-population growth–reproduction correlations.

Tab. S10 Summary of the primary rma model testing the effects of climate and functional traits on growth-reproduction relationships.

Tab. S11 Summary of the complementary rma model testing the effects of climate and functional traits on growth-reproduction relationships.

Tab. S12 Summary of the primary rma model testing the effect of interaction between mean CVp of seed production and the final year of the study.

Tab. S13 Summary of the complementary rma model testing the effect of interaction between mean CVp of seed production and the final year of the study.

Fig. S1 Decision tree.

Fig. S2 PRISMA flow chart.

Fig. S3 Category-dependent differences in population-level, within-year growth-reproduction correlations.

Fig. S4 Correlation between secondary growth and reproduction mapped on time-calibrated tree.

Fig. S5 Correlation between secondary growth and reproduction mapped on synthetic tree.

Fig. S6 Number of population-level seed-production time series used to estimate mean CVp.

Fig. S7 Funnel plot.

Fig. S8 Orchard plot based on the synthetic tree.

Fig. S9 Relationships between variables and mean Z values (effect sizes) used in the rma model testing the effects of climate and traits on growth–reproduction correlations.

Fig. S10 Sensitivity of the interaction between mean CVp of seed production and the final year

of the study to taxonomic composition.

Fig. S11 Temporal change in growth-reproduction correlations at contrasting levels of reproductive variability.

Fig. S12 Coverage of species-level functional traits investigated in the meta-analysis.

Supporting Information

Article title: Growth–reproduction trade-offs are common but changing in woody plants: a meta-analysis

Authors: Maciej K. Barczyk, Michał Bogdziewicz, Szymon M. Drobniak, Maria Bogdańska, Urszula Eichert, Jessie J. Foest, Valentin Journé, Katarzyna Kondrat, Jakub Szymkowiak, Andrew Hacket-Pain

Article acceptance date: 8 October 2026

Table S1: Search summary. Each row contains the set of keywords used for searching in the databases and the numbers of research items detected in the respective database. The trial search was performed on 22.03.2024. The final string was rerun on 30.03.2024 and supplied the meta-analysis (see Methods).

String	Scopus	Web of Science
(reproduction OR seed* OR cone* OR acorn*) AND (growth OR ring*) AND tree	23,244	22,733
(reproduction OR seed* OR cone* OR acorn* OR fruit*) AND (growth OR ring*) AND tree	33,863	32,367
(reproduction OR seed OR seeds OR fruit* OR cone* OR acorn*) AND ("tree growth" OR ring*) AND (tree* OR shrub*)	3,102	3,253

Table S2: Summary of the primary rma model testing the growth-reproduction relationships in relation to the different data categories. The effect sizes are based on the phylogenetically informed multilevel meta-analytic model accounting for random effects of **time-calibrated phylogeny**, study, and effect size ID. Primary and secondary growth were compared with other growth measurements (three-level factor); flowers, seeds and fruits were compared with all reproductive organs (three-level factor); populations were contrasted with meta-populations (two-leveled factor) and gymnosperms were compared with angiosperms (two-leveled factor) in a joint rma model, as visualized in the Fig. S3. The results are based on 308 observations derived from 78 studies on 79 species. Asterisks indicate significant effects. AIC = 193.76; I^2 = 62.94; R^2_m = 0.12. The estimated variance components of random effects equal 0.06 (~55%) for phylogeny, 0.05 (~45%) for study, and <0.001 (<1%) for effect size ID.

Predictor	estimate	se	z-value	p-value	ci.lb	ci.ub	
Intercept	-1.259	0.45	-2.798	0.005	-2.142	-0.376	**
Primary growth	0.955	0.396	2.415	0.016	0.18	1.73	*
Secondary growth	1.119	0.383	2.917	0.004	0.367	1.87	**
Population	-0.089	0.084	-1.062	0.288	-0.254	0.075	
Flowers	0.084	0.242	0.346	0.73	-0.391	0.559	
Seeds and fruits	0.07	0.208	0.336	0.737	-0.338	0.478	
Gymnosperms	-0.114	0.195	-0.586	0.558	-0.497	0.268	

Table S3: Summary of the complementary rma model testing the growth-reproduction relationships in relation to the different data categories. The effect sizes are based on the phylogenetically informed multilevel meta-analytic model accounting for random effects of **phylogeny from the synthetic tree**, study and effect size ID. Primary and secondary growth were compared with other growth measurements (three-level factor); flowers, seeds and fruits were compared with all reproductive organs (three-level factor); populations were contrasted with meta-populations (two-leveled factor) and gymnosperms were compared with angiosperms (two-leveled factor) in a joint rma model. The results are based on 308 observations derived from 78 studies on 79 species. Asterisks indicate significant effects. AIC = 193.93; I^2 = 69.08; R^2_m = 0.1. The estimated variance components of random effects equal 0.09 (~65%) for phylogeny, 0.05 (~<35%) for study, and <0.001 (<1%) for effect size ID.

Predictor	estimate	se	z-value	p-value	ci.lb	ci.ub	
Intercept	-1.227	0.46	-2.666	0.008	-2.129	-0.325	**
Primary growth	0.944	0.402	2.349	0.019	0.156	1.732	*
Secondary growth	1.099	0.39	2.817	0.005	0.334	1.863	**
Population	-0.085	0.084	-1.013	0.311	-0.248	0.079	
Flowers	0.088	0.241	0.364	0.716	-0.385	0.56	
Seeds and fruits	0.068	0.204	0.332	0.74	-0.332	0.467	
Gymnosperms	-0.135	0.213	-0.633	0.527	-0.552	0.282	

Table S4: Effect size formulas. Statistical tests and equations used to calculate standardized Pearson's r correlation coefficient. Intermediate effect size (t-value) was calculated with the use of respective effect size (ES) and standard error (SE) prior to conversions to Pearson's r coefficients following $t = ES/SE$. The n refers to the sample size.

Statistical test	Formula
t-test	$r_P = \sqrt{t^2/(t^2 + n - 1)}$
Spearman correlations	$r_P = 2\sin(\pi r_S/6)$
Linear models	$r_P = \sqrt{(t^2/(t^2 + n - 1)}$
Multiple regressions	$r_P = \sqrt{t^2/(t^2 + n - 2)}$

Table S5: Descriptive estimates of Pagel's λ and Blomberg's K for functional traits in the sampled species. The Pagel's λ (lambda) and Blomberg's K were calculated separately for each trait and species based on the time-calibrated phylogeny. Species-level data on plant height, seed mass, SLA (specific leaf area) were available for all 79 study species. Data on wood density was available for 61 species and for remaining 18 species it was averaged using the genus-level values.)

Functional trait	Pagel's λ	p-value		Blomberg's K	p-value	
Plant height	0.97	<0.001	***	0.054	<0.001	***
Seed mass	0.99	<0.001	***	0.019	<0.001	***
SLA	0.99	<0.001	***	0.017	0.06	
Wood density	0.60	<0.001	***	0.009	0.002	**

Table S6: Estimated mean growth–reproduction correlations across three temporal alignments in the primary meta-analytic model. The effect sizes are based on phylogenetically informed multilevel meta-analytic model without an intercept accounting for random effects of **time-calibrated phylogeny**, study, and effect size ID. The results are based on 685 observations and 79 species (Fig. 2B). Asterisks indicate significant effects. AIC = 444.53; I^2 = 42.14, R^2_m = 0.35. The estimated variance components of random effects equal 0.015 (~36%) for phylogeny, <0.001 for study (<1%), and 0.026 (~64%) for effect size ID.

Predictor	estimate	se	z-value	p-value	ci.lb	ci.ub	
Lagged effect ($t + 1$)	0.007	0.069	0.096	0.923	-0.128	0.142	
Unlagged effect (t)	-0.231	0.067	-3.45	<0.001	-0.362	-0.1	***
Lagged effect ($t - 1$)	0.108	0.068	1.581	0.114	-0.026	0.242	

Table S7: Estimated mean growth–reproduction correlations across three temporal alignments in the complementary meta-analytic model. The effect sizes are based on phylogenetically informed multilevel meta-analytic model without an intercept accounting for random effects of **phylogeny from the synthetic tree,** study, and effect size ID. The results are based on 685 observations and 79 species (Fig. S8). Asterisks indicate significant effects. AIC = 443.63; I^2 = 37.19; R^2_m = 0.40. The estimated variance components of random effects equal <0.001 (<1%) for phylogeny, 0.008 (~24%) for study, and 0.026 (~76%) for effect size ID.

Predictor	estimate	se	z-value	p-value	ci.lb	ci.ub	
Lagged effect ($t + 1$)	0.039	0.03	1.304	0.192	-0.02	0.097	
Unlagged effect (t)	-0.199	0.024	-8.388	<0.001	-0.245	-0.152	***
Lagged effect ($t - 1$)	0.143	0.028	5.120	<0.001	0.088	0.198	***

Table S8: Summary of the primary rma model testing the relationships between the within-population growth–reproduction correlations (Z-score) in the same year (t), and correlations in the preceding ($t-1$) and the following ($t+1$) year. The effect sizes are based on phylogenetically informed multilevel meta-analytic model accounting for random effects of **time-calibrated phylogeny**, study, and effect size ID. The results are based on 172 observations and 51 species for which information on population-level correlation was available (Fig. 2C,D). Asterisks indicate significant effects. AIC = 26.02; I^2 = 48.82; R^2_m = 0.16. The estimated variance components of random effects equal <0.001 (<1%) for phylogeny, 0.05 (~100%) for study, and <0.001 (<1%) for effect size ID.

Predictor	estimate	se	z-value	p-value	ci.lb	ci.ub	
Intercept	-0.107	0.056	-1.924	0.054	-0.2161	0.002	
Lagged effect ($t-1$) Z	-0.253	0.079	-3.219	0.001	-0.407	-0.099	**
Lagged effect ($t+1$) Z	-0.166	0.098	-1.702	0.089	-0.357	0.025	

Table S9: Summary of the complementary rma model testing the relationships between the within-population growth–reproduction correlations (Z-score) in the same year (t), and correlations in the preceding ($t-1$) and the following ($t+1$) year. The effect sizes are based on phylogenetically informed multilevel meta-analytic model accounting for random effects of **phylogeny from the synthetic tree**, study, and effect size ID. The results are based on 172 observations and 51 species for which information on population-level correlation was available. Asterisks indicate significant effects. AIC = 26.02; I^2 = 48.82; R^2_m = 0.16. The estimated variance components of random effects equal <0.001 (<1%) for phylogeny, 0.05 (~100%) for study, and <0.001 (<1%) for effect size ID.

Predictor	estimate	se	z-value	p-value	ci.lb	ci.ub	
Intercept	-0.107	0.056	-1.924	0.054	-0.2161	0.002	
Lagged effect ($t-1$) Z	-0.253	0.079	-3.219	0.001	-0.407	-0.099	**
Lagged effect ($t+1$) Z	-0.166	0.098	-1.702	0.089	-0.357	0.025	

Table S10: Summary of the primary rma model testing the effects of climate and functional traits on growth-reproduction relationships. The effect sizes are based on phylogenetically informed multilevel meta-analytic model accounting for random effects of **time-calibrated phylogeny**, study and effect size ID. MAT - Mean Annual Temperature, MAP - Mean Annual Precipitation, VPD - Vapor Pressure Deficit, SLA - Specific Leaf Area. The results are based on 308 observations and 79 species (Fig. 4). AIC = 204.67; I^2 = 61.52; R^2_m = 0.04. The estimated variance components of random effects equal 0.04 (~43%) for phylogeny, 0.05 (~57%) for study, and <0.001 (<1%) for effect size id.

Predictor	estimate	se	z-value	p-value	ci.lb	ci.ub
Intercept	-0.347	0.177	-1.957	0.05	-0.695	0.001
MAT	-0.048	0.051	-0.929	0.353	-0.148	0.053
MAP	0.01	0.033	0.312	0.755	-0.054	0.074
VPD	0.181	0.224	0.806	0.42	-0.259	0.62
SLA	-0.027	0.044	-0.61	0.542	-0.113	0.059
Wood density	-0.005	0.045	-0.121	0.904	-0.093	0.082
Plant height	-0.024	0.071	-0.335	0.738	-0.164	0.116
Seed mass	0.066	0.054	1.227	0.22	-0.04	0.172

Table S11: Summary of the complementary rma model testing the effects of climate and functional traits on growth-reproduction relationships. The effect sizes are based on phylogenetically informed multilevel meta-analytic model accounting for random effects of **phylogeny from the synthetic tree**, study, and effect size ID. MAT - Mean Annual Temperature, MAP - Mean Annual Precipitation, VPD - Vapor Pressure Deficit, SLA - Specific Leaf Area. The results are based on 308 observations and 79 species. AIC = 203.43; I^2 = 66.18; R^2_m = 0.04. The estimated variance components of random effects equal 0.06 (~55%) for phylogeny, 0.05 (~45%) for study, and <0.001 (<1%) for effect size id.

Predictor	estimate	se	z-value	p-value	ci.lb	ci.ub
Intercept	-0.312	0.194	-1.604	0.109	-0.692	0.069
MAT	-0.029	0.051	-0.564	0.573	-0.129	0.072
MAP	0.008	0.033	0.25	0.803	-0.056	0.072
VPD	0.138	0.224	0.617	0.537	-0.302	0.578
SLA	-0.026	0.043	-0.606	0.545	-0.111	0.059
Wood density	-0.031	0.046	-0.662	0.508	-0.121	0.06
Plant height	-0.067	0.073	-0.924	0.356	-0.21	0.075
Seed mass	0.078	0.054	1.454	0.146	-0.027	0.183

Table S12: Summary of the primary rma model testing the effect of interaction between mean CV_p of seed production and the final year of the study. The effect sizes are based on phylogenetically informed multilevel meta-analytic model accounting for random effects of **time-calibrated phylogeny**, study, and effect size ID. Asterisks indicate significant effects. The results are based on 261 observations and 48 species for which CV_p values were available (Fig 5A). Asterisks indicate significant effects. AIC = 148.19; I^2 = 52.78; R^2_m = 0.14. The estimated variance components of random effects equal 0.04 (~57%) for phylogeny, 0.03 (~43%) for study, and <0.001 (<1%) for effect size id.

Predictor	estimate	se	z-value	p-value	ci.lb	ci.ub	
Intercept	41.97	16.678	2.517	0.012	9.282	74.657	*
Mean CV_p	-41.337	12.634	-3.272	0.001	-66.1	-16.575	**
Final year of the study	-0.021	0.008	-2.522	0.012	-0.037	-0.005	*
Mean CV_p : Final year	0.021	0.006	3.264	0.001	0.008	0.033	**

Table S13: Summary of the complementary rma model testing the effect of interaction between mean CV_p of seed production and the final year of the study. The effect sizes are based on phylogenetically informed multilevel meta-analytic model accounting for random effects of **phylogeny from the synthetic tree**, study and effect size ID. Asterisks indicate significant effects. The results are based on 261 observations and 48 species for which CV_p values were available. Asterisks indicate significant effects. AIC = 142.61; I^2 = 64.02; R^2_m = 0.11. The estimated variance components of random effects equal 0.09 (~81%) for phylogeny, 0.02 (~19%) for study, and <0.001 (<1%) for effect size id.

Predictor	estimate	se	z-value	p-value	ci.lb	ci.ub	
Intercept	42.64	15.9	2.682	0.007	11.477	73.803	**
Mean CV_p	-42.778	12.148	-3.522	<0.001	-66.587	-18.969	***
Final year of the study	-0.021	0.008	-2.687	0.007	-0.037	-0.006	**
Mean CV_p : Final year	0.021	0.006	3.512	<0.001	0.009	0.033	***

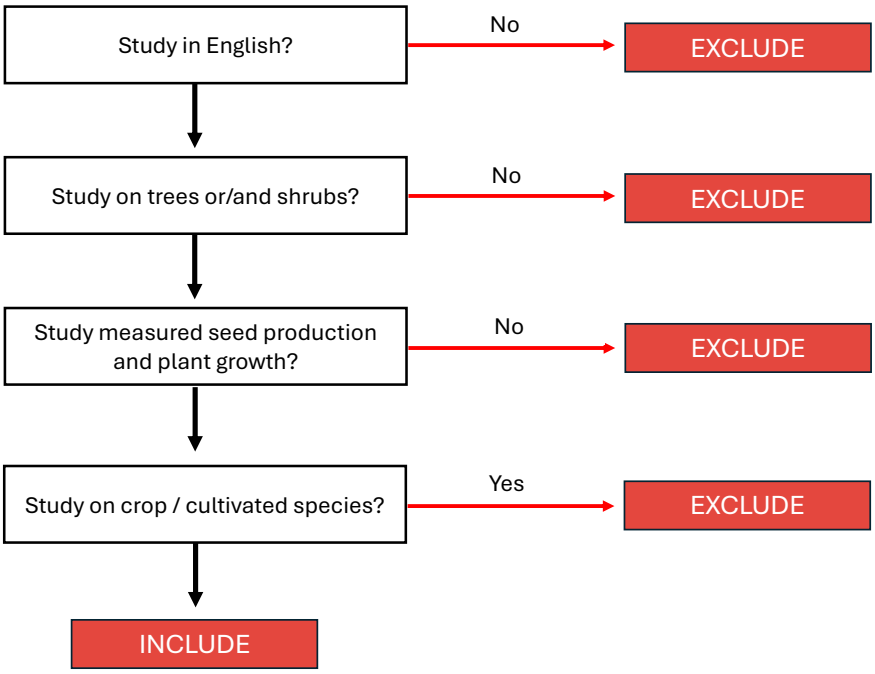


Figure S1: Decision tree. Decision tree with the inclusion criteria used in meta-analysis.

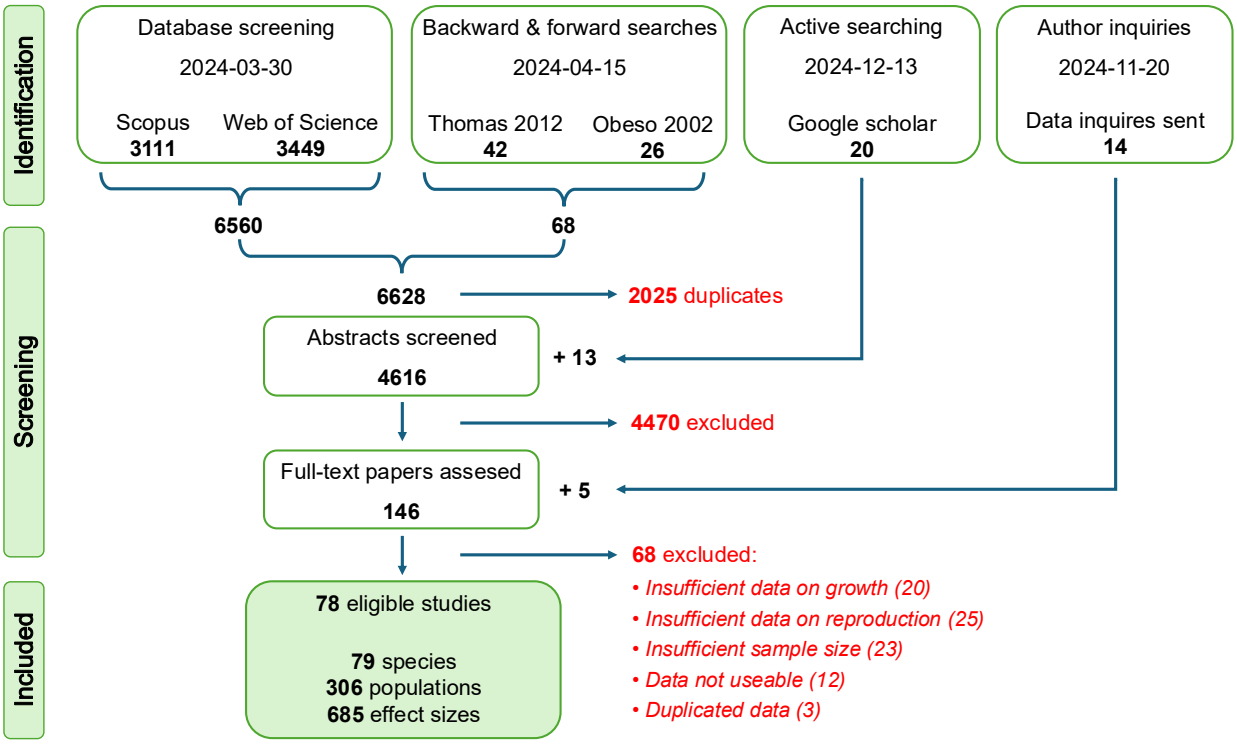


Figure S2: PRISMA flow chart. PRISMA graph summarizes the methods and data used in meta-analysis, including the search description, number of screened and excluded studies, the reasons for exclusion, and the final details on eligible studies.

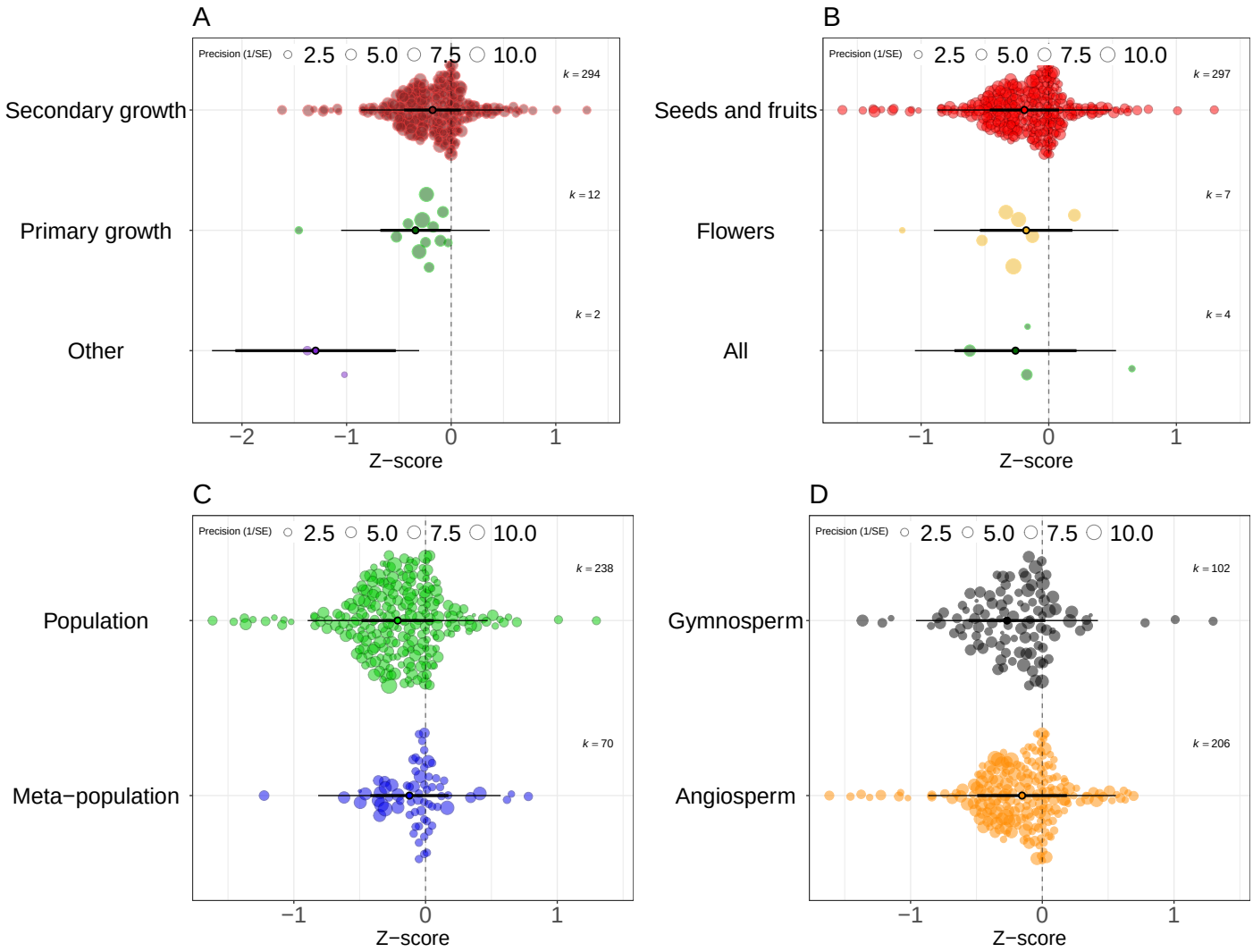


Figure S3: Category-dependent differences in population-level, within-year growth-reproduction correlations. A) Comparison of the effect sizes (Z-score) between different growth measurements. Secondary growth measurements derive mostly from tree ring data and basal area increments. Primary growth refers to measurements of buds, twigs, organs or plant height increments. Other methods ("others") refer to two studies using photosynthetic capacity [O evolution/leaf area] and root collar non-stuctural carbohydrate (NSC) levels as growth proxy. B) Comparison of the effect sizes (Z-score) between different reproduction measurements. C) Comparison of the effect sizes (Z-score) between populations and meta-populations. D) Comparison of the effect sizes (Z-score) between gymnosperms and angiosperms. Model summary provided in Table S2.

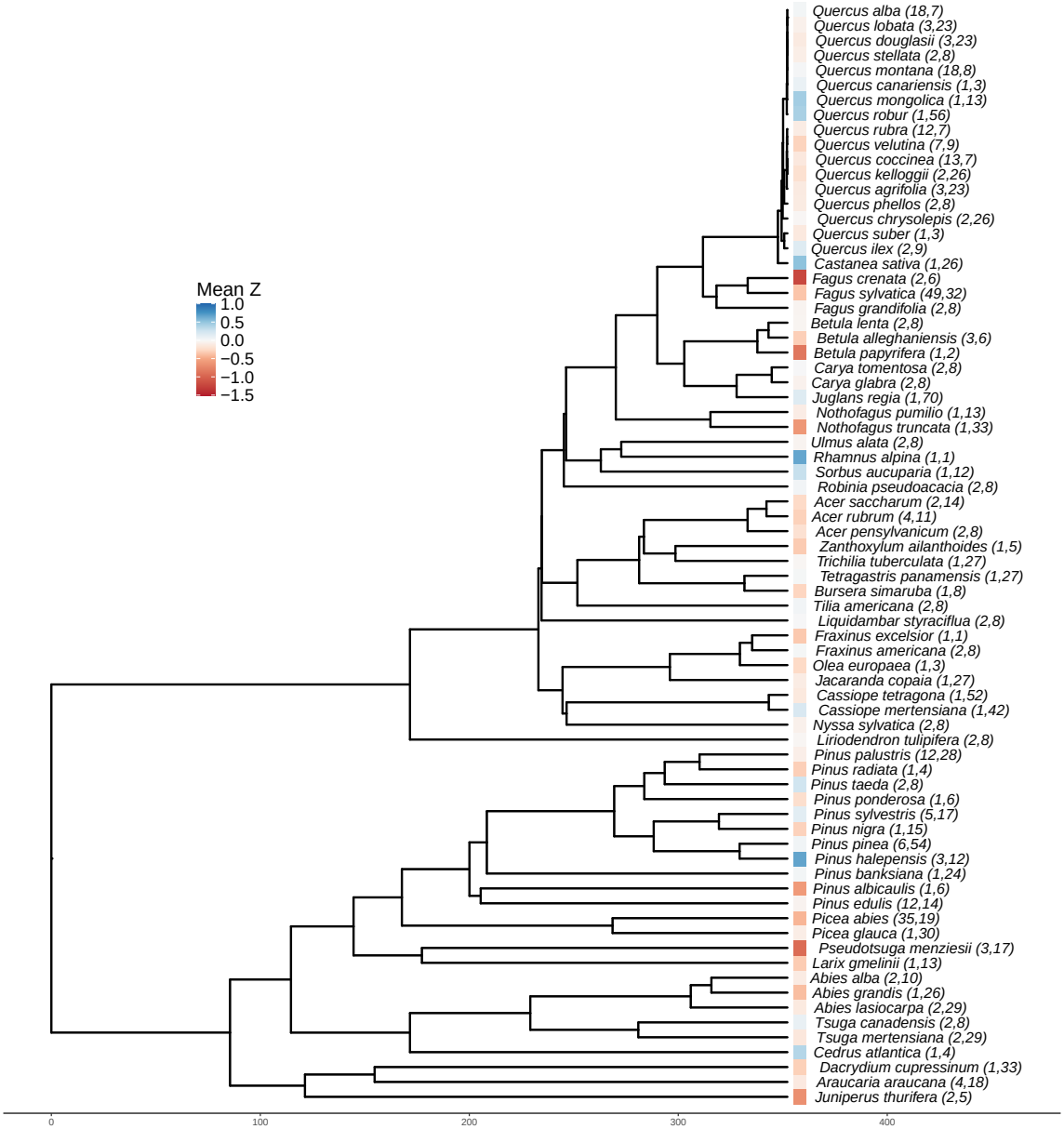


Figure S4: Correlation between secondary growth and reproduction mapped on time-calibrated tree. Warmer colors (reds) indicate negative, and cooler colors (blues) indicate positive correlations between reproduction and growth in the same year (t). In brackets given are: the number of populations in which trade-offs were studied and the mean number of years for each species. The branch lengths reflect the evolutionary distances measured in millions of years (see the bar with the scale below). Phylogenetic signal is: Pagel's $\lambda < 0.001$, $p = 0.99$, Blomberg's K = 0.015, $p = 0.003$, $n = 74$ species. The data is restricted to the observations derived from studies measuring secondary growth only (see Fig. S3).

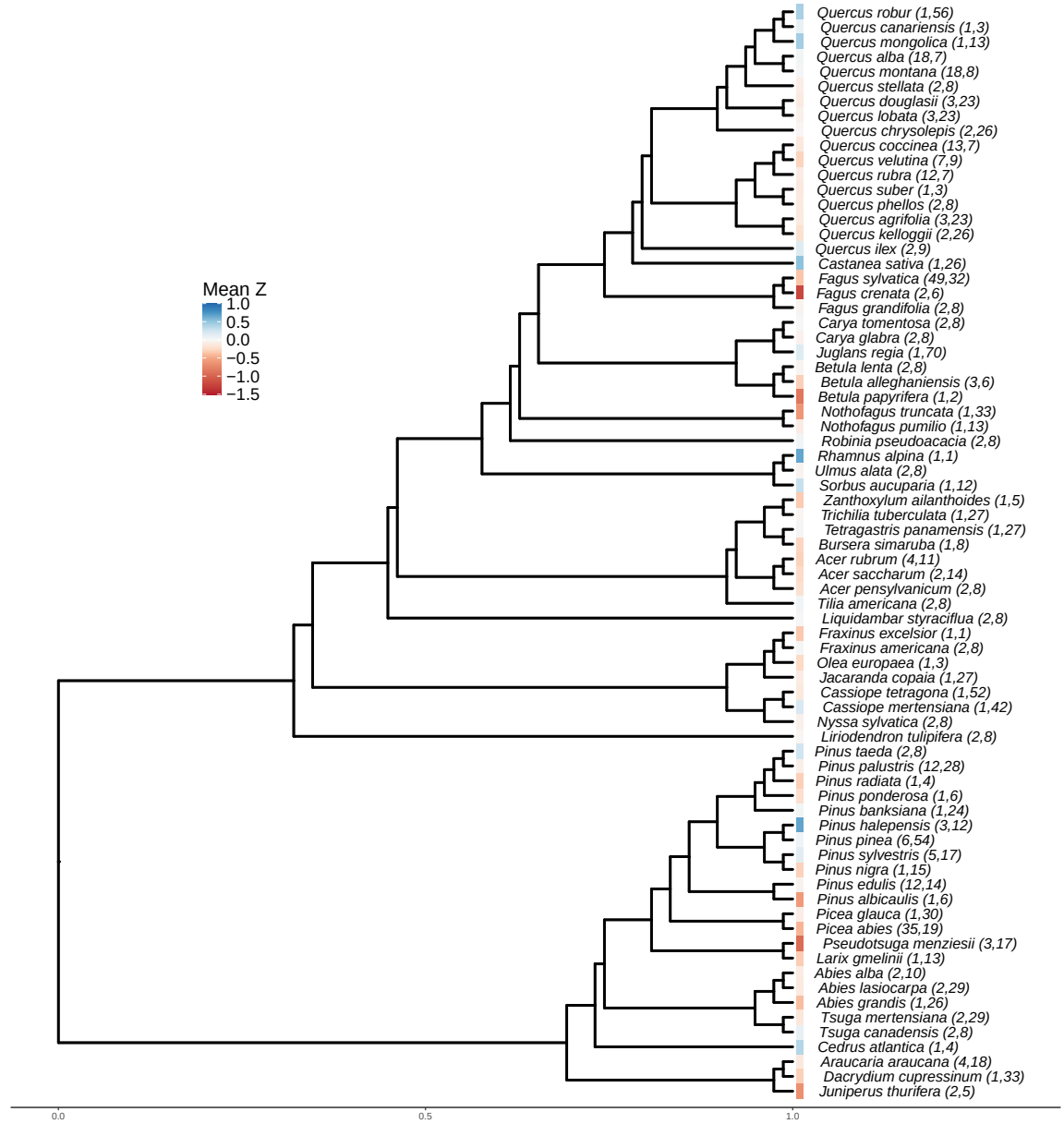


Figure S5: Correlation between secondary growth and reproduction mapped on synthetic tree. Warmer colors (reds) indicate negative, and cooler colors (blues) indicate positive correlations between reproduction and growth in the same year (t). In brackets given are: the number of populations in which trade-offs were studied and the mean number of years for each species. The branch length was calculated with the Grafen's method and does not reflect the absolute time of the divergence between clades. Phylogenetic signal is: Pagel's $\lambda < 0.001$, $p = 0.99$, Blomberg's $K = 0.054$, $p = 0.09$, $n = 74$ species. The data is restricted to the observations derived from studies measuring secondary growth only.

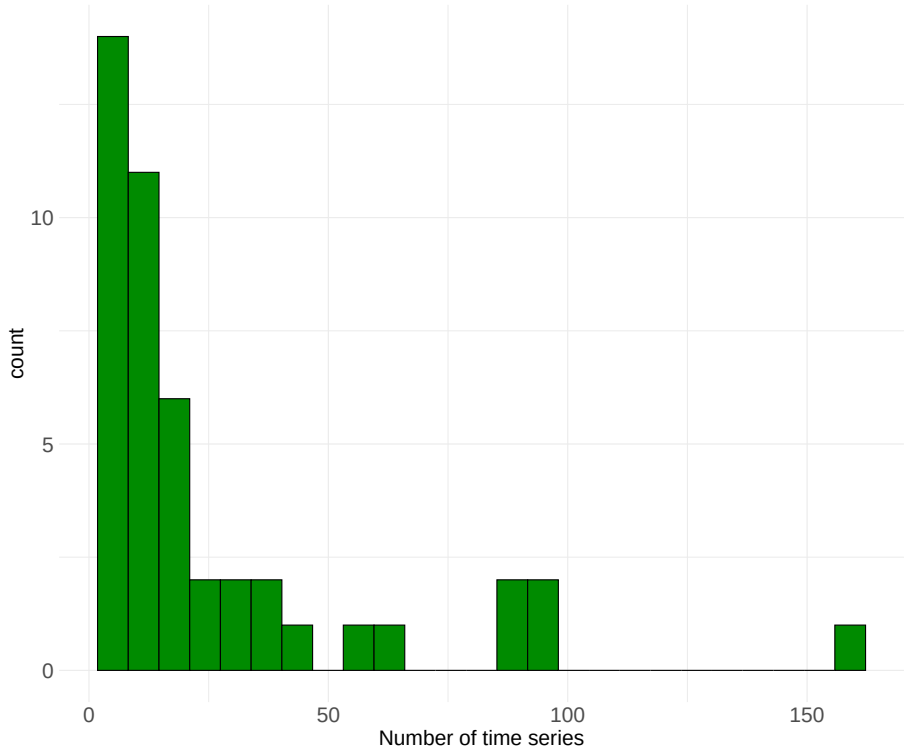


Figure S6: Number of population-level seed-production time series used to estimate mean CVp of 48 species from the meta-analysis. Species-level estimates were based on a minimum of five population-level time series (n >= 5 years) per species.

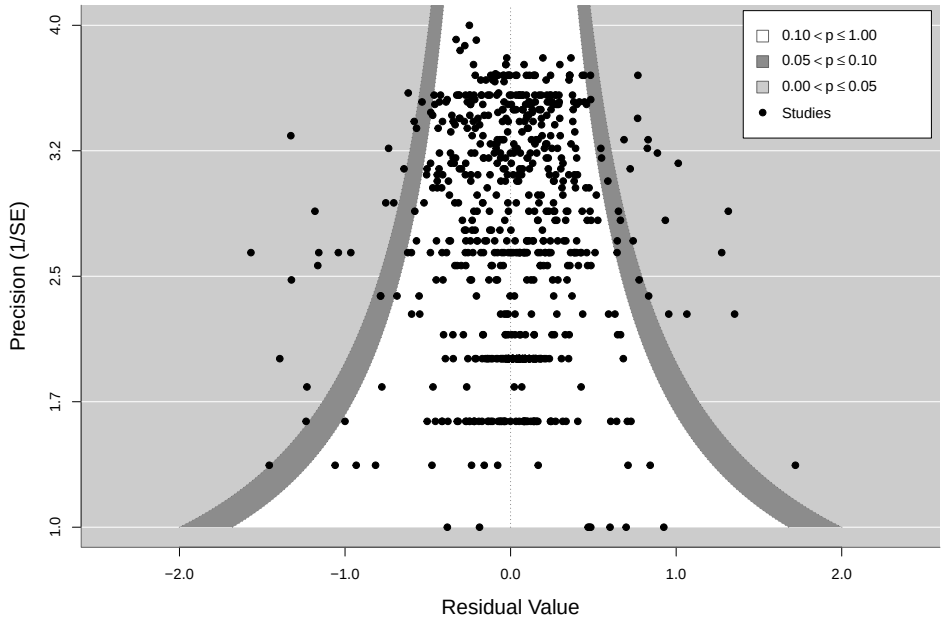


Figure S7: Funnel plot. Residual values from the rma model are plotted in relation to their precision (inverse standard error). Each point refers to population-level growth-reproduction correlation (based on all time lags, n = 685, Fig. 2B). The model included the square root of sampling variance as the main predictor, and species, study and effect size ID as random effects. Shades highlight different levels of statistical significance described in the legend.

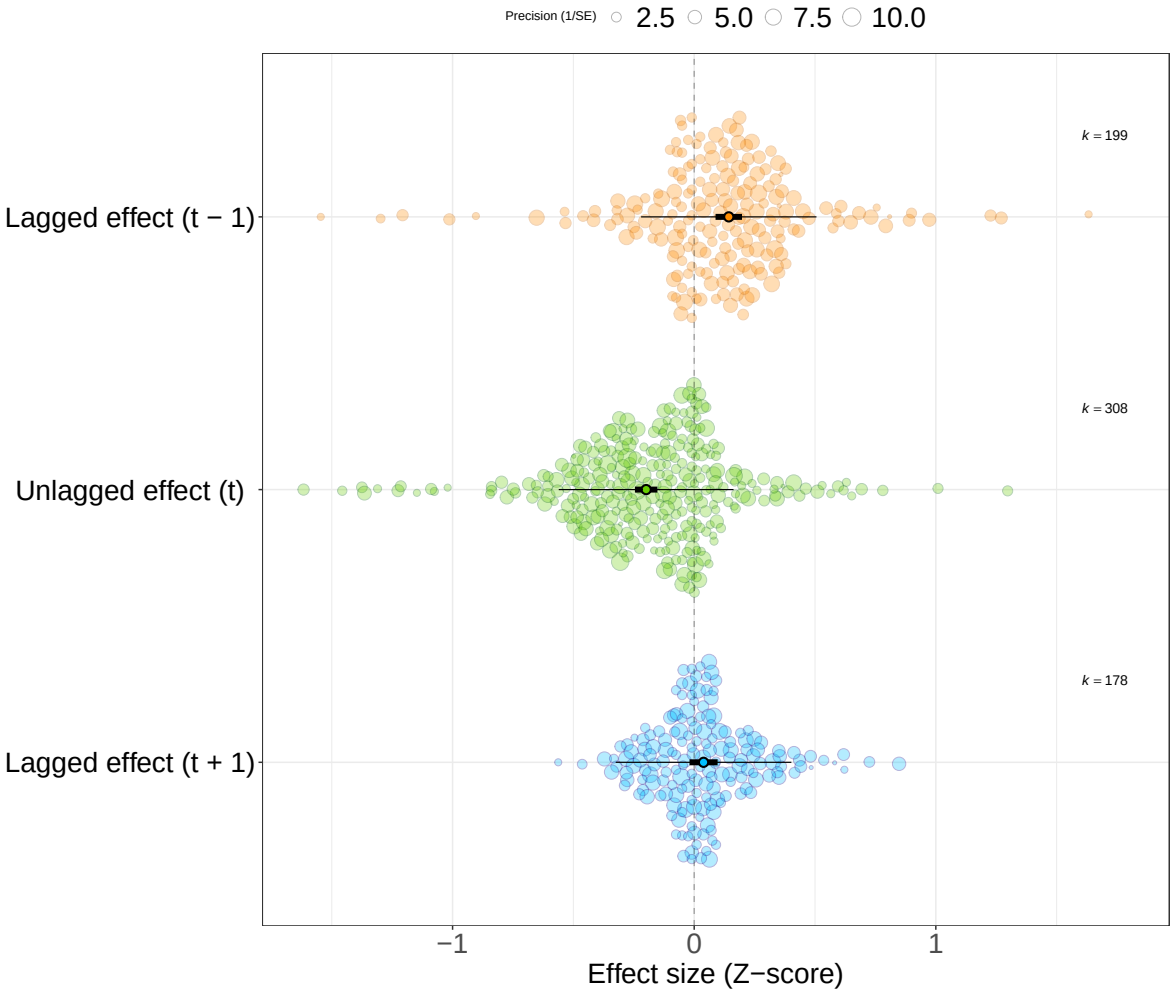


Figure S8: Growth is higher in years preceding seed production, reduced in years of high seed production, and suppressed in years following seed production. Relationships between reproduction and growth in the preceding year ($t-1$), same year (t), and the subsequent year ($t+1$). The effect sizes are based on phylogenetically informed multilevel meta-analytic model without an intercept accounting for random effects of **phylogeny from the synthetic tree**, study, and effect size ID. Black points show estimated effect sizes with 95% confidence intervals (CI; thicker bars) and 95% prediction intervals (PI; thinner bars). Points represent population-level effect sizes (k), with point size proportional to their precision (inverse SE). Model summary provided in Table S7.

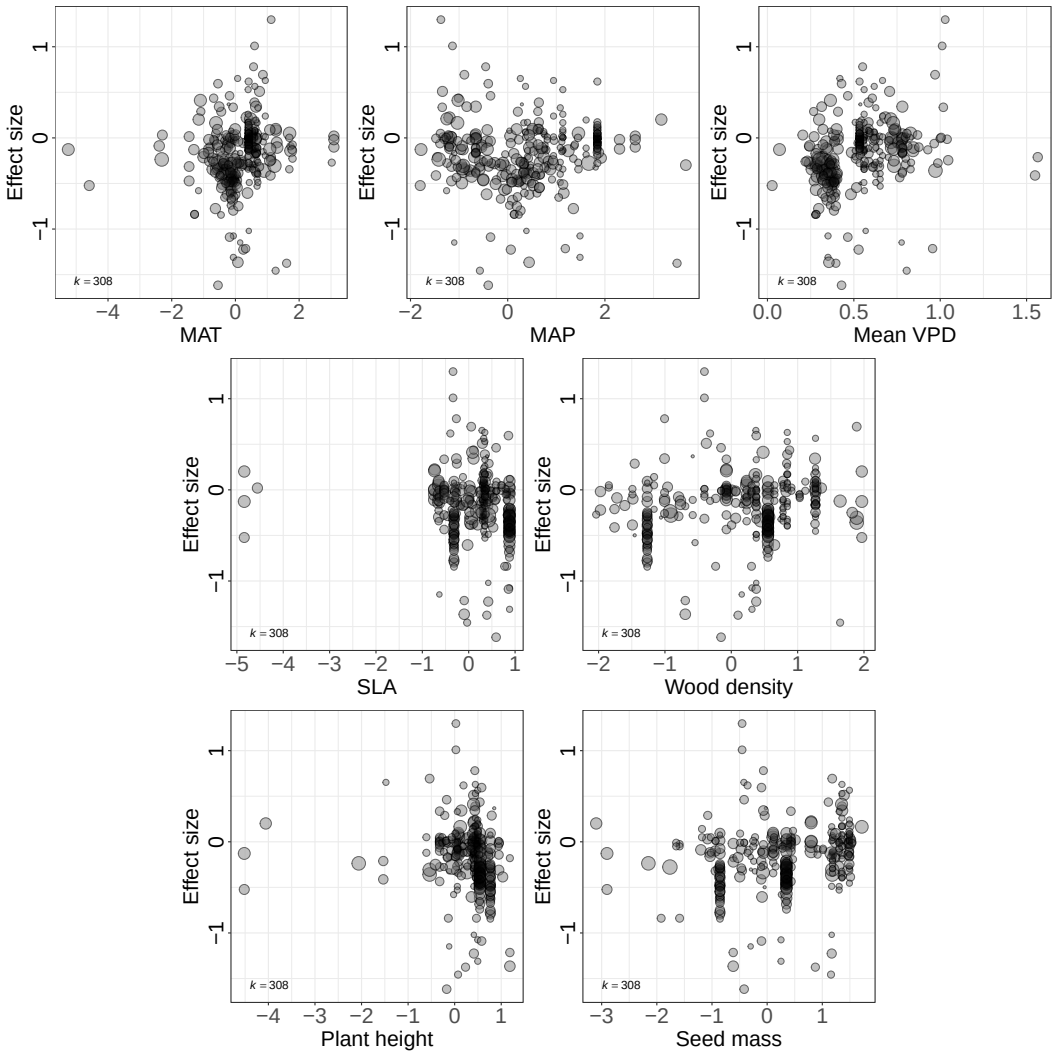


Figure S9: Relationships between variables and mean Z values (effect sizes) used in the rma model testing the effects of climate and traits on growth–reproduction correlations. Each window represents one studied variable tested in the meta-analysis (i.e. mean annual temperature, mean annual precipitation, mean vapor deficit pressure, specific leaf area, wood density, plant height, seed mass; see Fig. 4). Points represent population-level effect sizes (k), with point size proportional to their precision (inverse SE).

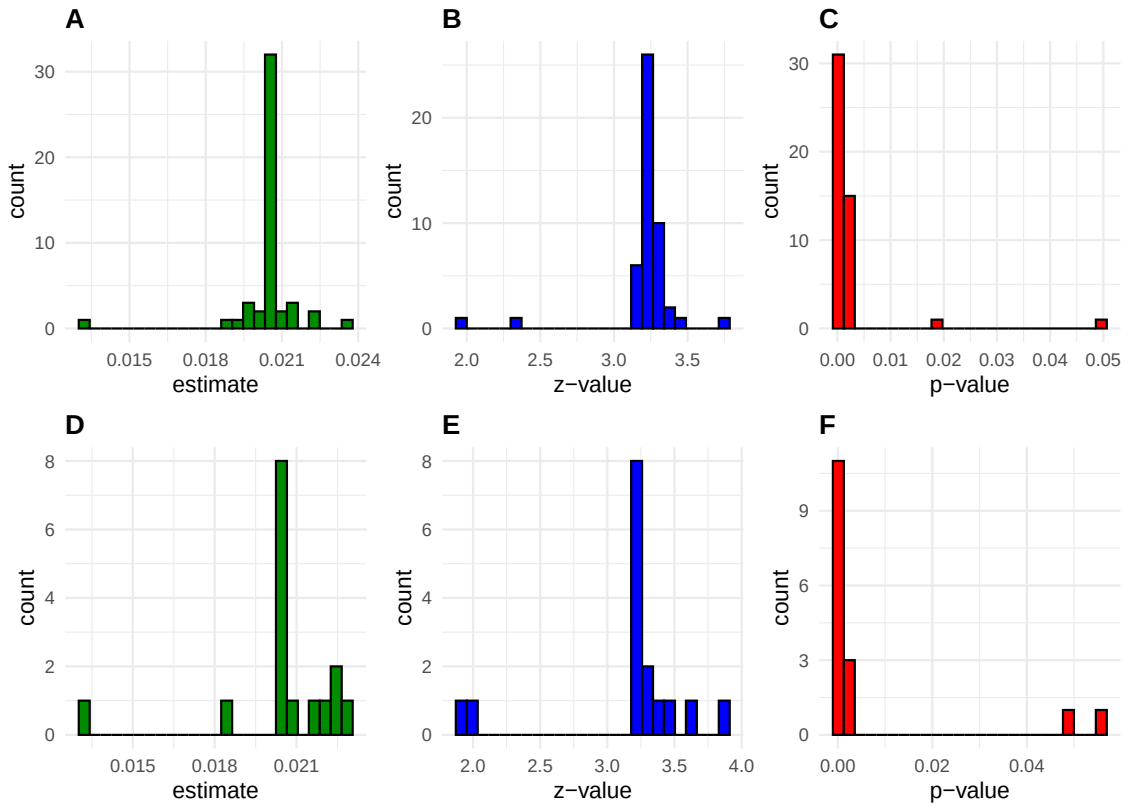


Figure S10: Sensitivity of the interaction between mean CVp of seed production and the final year of the study to taxonomic composition. Histograms show the coefficient estimates, z-values, and p-values obtained after sequentially excluding each species (48 models; first row) or each genus (16 models; second row) from the dataset. The interaction remained positive and statistically significant ($p < 0.05$) in all refitted models. All models otherwise followed the structure of the full model presented in Table S12).

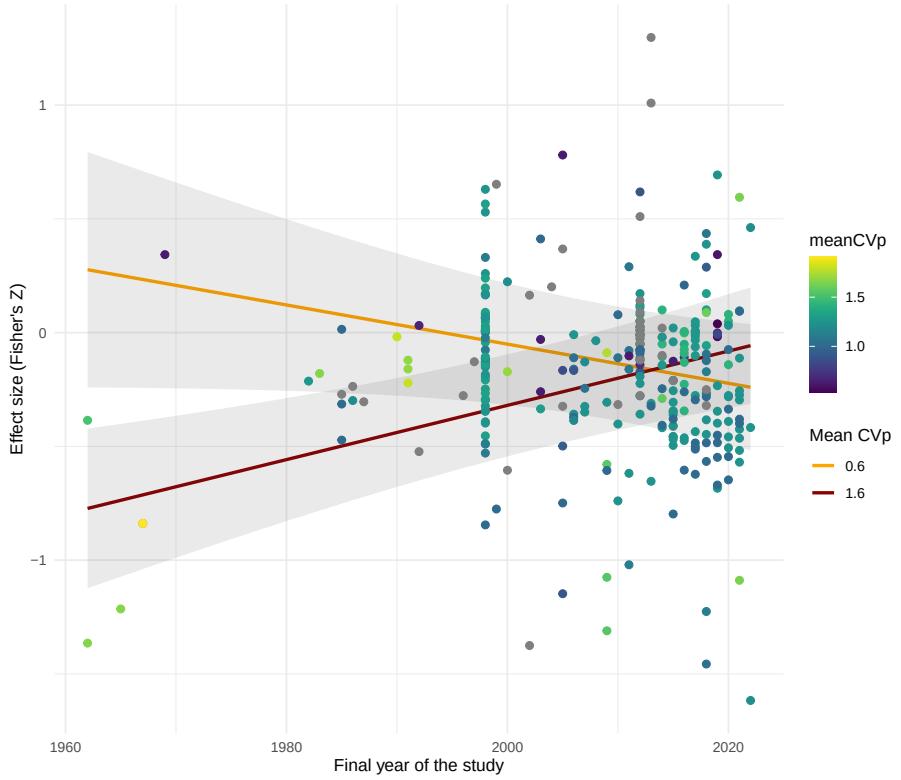


Figure S11: Temporal change in growth-reproduction correlations at contrasting levels of reproductive variability. Points show observed population-level Fisher's Z effect sizes and are colored by species-level mean CV_p. Lines and shaded 95% confidence intervals show predictions from the continuous final-study-year × mean CV_p meta-regression (see Table S12), evaluated at mean CV_p values of 0.6 and 1.6. These values were used only to visualize the interaction.

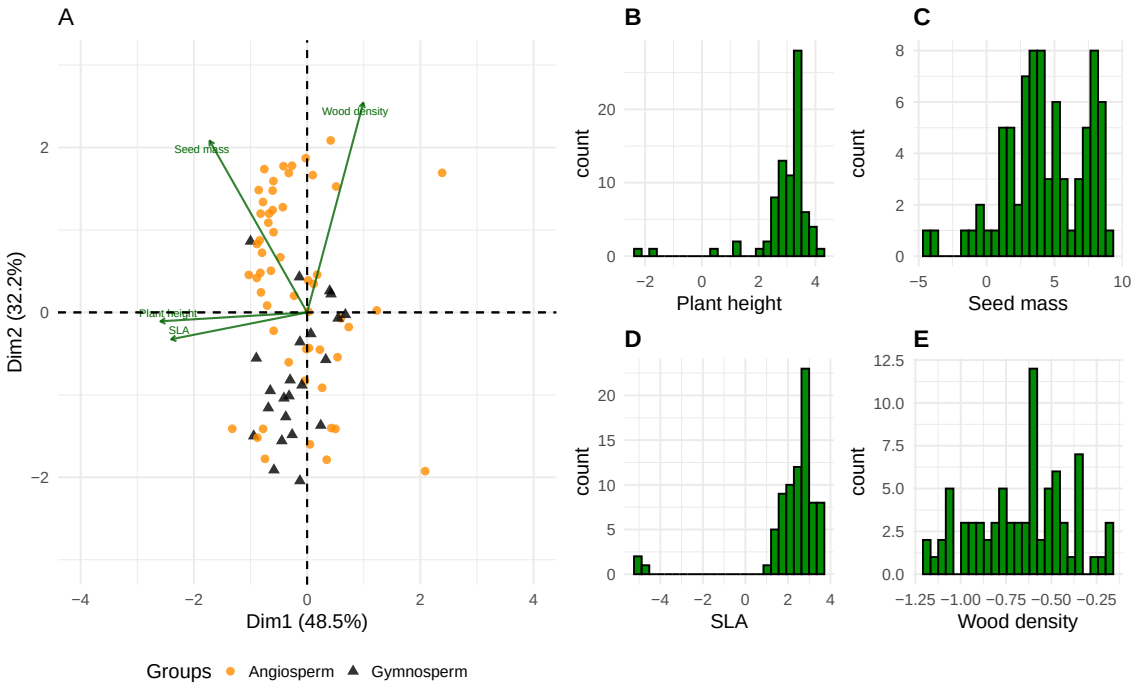


Figure S12: Coverage of species-level functional traits investigated in the meta-analysis. A) Principal Component Analysis. Arrow length indicate relationships between four functional traits tested in the meta-analysis (i.e. SLA, plant height, wood density, seed mass) (Fig. 4) averaged at the species level (n = 79). Each point represents single species (yellow - angiosperms, black triangles - gymnosperms). B) Histogram of log-transformed plant height. C) Histogram of log-transformed seed mass. D) Histogram of log-transformed SLA (specific leaf area). E) Histogram of log-transformed wood density (including genus-level average values).